

High-Redshift Galaxy Surveys and the Reionization of the Universe

Rychard Bouwens

Abstract Star-forming galaxies in the early universe provide us with perhaps the most natural way of explaining the reionization of the universe. Current observational results are sufficiently comprehensive, as to allow us to approximately calculate how the ionizing radiation from galaxies varies as a function of cosmic time. Important uncertainties in modeling reionization by galaxies revolve around the escape fraction and its luminosity and redshift dependence, a possible truncation of the galaxy luminosity function at the faint end, and an evolution in the production efficiency of Lyman-continuum photons with cosmic time. Despite these uncertainties, plausible choices for these parameters naturally predict a cosmic ionizing emissivity at $z \sim 6$ -10 whose evolution and overall normalization is in excellent agreement with that derived from current observational constraints. This strongly suggests that galaxies provide the necessary photons to reionize the universe.

1 Introduction

One of the most important questions in observational cosmology regards the reionization of the neutral hydrogen in the universe. Over what time scale did reionization occur and which sources caused it? Observationally, we have constraints on reionization from the Gunn-Peterson trough in luminous high-redshift quasars [1, 2], the Thomson optical depths observed in the Microwave background radiation [3], and the luminosity function and clustering properties of Ly α emitters [e.g., 4]. Reionization appears to have begun at least as early as $z \sim 11$ [5], with a midpoint at $z \sim 9$, and finished no later than $z \sim 6$ [e.g., 4, 2, 6, 7].

Due to the low volume densities of QSOs at high redshift [e.g., 8, 9] and the lack of compelling evidence for other ionizing sources (e.g., self-annihilating dark mat-

Rychard Bouwens
Leiden Observatory, Niels Bohrweg 2, Leiden NL2333, Netherlands, e-mail: bouwens@strw.leidenuniv.nl

ter or mini-quasars: [10, 11]), star-forming galaxies represent the most physically well-motivated source of ionizing photons. Observational surveys of galaxies in the distant universe therefore provide us with our best guide to mapping how the volume density of ionizing radiation likely varies with both redshift and cosmic time.

Fortunately, current surveys of the distant universe continue to provide us with better constraints on the volume density of galaxies over a wide range in luminosity and redshift [e.g., 12, 13]. Both very sensitive observations with the Hubble Space Telescope and wide field observations from ground-based instruments are key to obtaining these improved constraints on the volume densities. Quantifying the volume density of ultra-faint galaxies is particularly important for determining the impact of galaxies to reionizing the universe.

2 Galaxies as a Potential Source of the Cosmic Ionizing Emissivity

Obtaining direct constraints on the ionizing UV radiation from galaxies escaping into the intergalactic medium is quite difficult. Direct detection of this radiation can barely be done for galaxies at $z \sim 1-3$ or even in the nearby universe. For galaxies at $z \geq 6$ where reionization occurs, this endeavor is exceedingly challenging, as any ionizing radiation must first redshift through the dense Lyman-series forest in the high-redshift universe prior to any attempted observation. Indirect methods, such as use of the proximity effect [14, 15], to constrain the ionizing radiation from galaxies may hold some promise, but that technique has largely been used in the context of such radiation from quasars.

Because of the difficulties in setting direct constraints on the total ionizing radiation coming from galaxies, astronomers try to estimate this total as the product of three quantities, the rest-frame *UV* luminosity density ρ_{UV} , an efficiency factor in converting the *UV* luminosity to Lyman-continuum emission ξ_{ion} , and the escape fraction f_{esc} . Existing observations allow us to place firm lower limits on the first of these quantities, the *UV* luminosity density ρ_{UV} , while the third quantity here, the escape fraction f_{esc} , is much more difficult to accurately constrain. The escape fraction can be defined in a variety of ways but roughly expresses the relative fraction of Lyman-continuum-ionizing photons escaping from galaxies to the fraction of *UV*-continuum photons which escape.

2.1 *UV*-continuum Luminosity Density

Of those quantities relevant to galaxy's role in reionizing the universe, the most straightforward quantity to constrain is the rest-frame *UV* luminosity density ρ_{UV} . This density quantifies the total luminosity of galaxies at *UV*-continuum wavelengths in a given comoving volume of the universe.

To quantify the luminosity density ρ_{UV} at a given epoch, astronomers take the volume density of galaxies they derive from searches for galaxies as a function of luminosity (i.e., the UV luminosity function), multiply this volume density by the luminosity, and then integrate this product over the full range of observed (and expected) galaxy luminosities:

$$\rho_{UV} = \int_{L_{min}}^{L_{max}} \phi(L) L dL \quad (1)$$

where L is the UV luminosity of galaxies, $\phi(L)$ is the volume density of galaxies as a function of luminosity, and L_{min} and L_{max} are the lowest and highest luminosities that galaxies can attain.

As is apparent from the equation above, deriving the UV luminosity density ρ_{UV} at a given epoch is nominally a very rudimentary calculation to perform, after one derives the UV luminosity function from one or more observational probes. In practice, however, this endeavor is not entirely straightforward, which is a direct consequence of the apparently large population of galaxies with luminosities fainter than what we can readily probe with existing data sets. Observationally, there is no credible evidence for a possible cut-off in the UV luminosity function towards the faint end of what can be currently observed. Additionally, from simple theoretical models, one could reasonably expect galaxies to efficiently form ~ 50 to $1000\times$ fainter than the current observational limits.

The importance of faint galaxies for driving the reionization of the universe lies in their large volume densities. Extrapolating the observed luminosity function to lower luminosities (e.g., -10 mag: $\sim 10^4$ fainter than L^* galaxies) suggest that these ultra-faint (and largely individually undetectable) galaxies could produce $\sim 7\times$ as much light as the galaxies that we can probe directly with currently observable surveys [e.g., 16] (Figure 3).

2.2 Evolution of the UV LF from Early Times

One particularly important aspect of ascertaining whether galaxies can be successful in reionizing the universe involves a characterization of their evolution with cosmic time. The rate of evolution can have a big impact on how luminous galaxies are in the early universe and this will affect how many ionizing photons they produce.

After more than 10 years of careful quantitative analyses of large samples of $z \sim 4-8$ galaxies, the evolution of the UV LF is now very well characterized over the redshift range $z \sim 4$ to $z \sim 8$. Essential for these analyses are the very sensitive, wide-area images of the distant universe in multiple wavelength channels, stretching from near-UV wavelengths into the infrared.

Due to the unique colors and spectral shape of young star-forming galaxies in the $z \geq 4$ universe, one can take advantage of the rich multi-wavelength information in deep imaging observations to identify large numbers of largely robust $z \sim 4-$

8 galaxies. The general technique used to identify distant galaxies is called the Lyman-break technique and has been demonstrated to work very efficiently from important pioneering work in the mid-1990s on galaxies at $z \sim 3$ [17, 18], with subsequent demonstrations on thousands of galaxies at $z = 3-6$ [e.g., 19, 20] to the current high-redshift record-holder $z = 7.73$ [21]. Application of techniques like the Lyman-break technique and more generally selections using photometric-redshift estimators to data both from large telescopes on the ground and from the Hubble Space Telescope [e.g., 22, 13] have made it possible to construct samples with extremely large numbers ($>10^4$) of galaxies.

The most valuable observations for constraining the luminosity functions are those that probe the volume density of the faintest sources and those that probe the volume density of the brightest sources. Constraints on the volume density of the faintest sources have typically come from the optical and near-infrared observations of the Hubble Ultra Deep Field (HUDF) with the Hubble Space Telescope with the Advanced Camera for Surveys Wide-Field Camera and the near-infrared channel on the Wide Field Camera 3. Most of the observations were obtained as part of the original HUDF campaign in 2004 [23] and as part of the HUDF09 and HUDF12 campaigns in 2009-2012 [24, 25]. These observations are effective in detecting sources to 30 AB mag, equivalent to a luminosity of -16 mag at $z \sim 4$ and -17 mag at $z \sim 7$ [26, 27, 28, 13]. Figure 1 shows one recent state-of-the-art compilation of LF determinations.

Constraints on the volume density of bright galaxies have predominantly come from two sources: (1) the wide-area (~ 900 arcmin²) optical and near-infrared observations from the Great Observatories Origins Deep Survey [GOODS: 29] and CANDELS program [30, 31] and (2) square-degree ground-based search fields like the UKIDSS Ultra Deep Survey, UltraVISTA [32], and the Canada-France-Hawaii Telescope deep legacy survey fields [22, 33]. These wide-area programs generally have been successful in finding a few very bright star-forming galaxies to $\sim 23-24$ mag. The search results have important implications for the build-up of bright galaxies and the evolution of the characteristic luminosity L^* , but do not have an especially meaningful impact on the overall background of ionizing photons in the *UV*.

Very good agreement is found between independent determinations of the rest-frame *UV* luminosity functions of galaxies at $z \sim 4-10$ [13, 34, 35, 36]. Most of the debate in the literature has revolved about how the evolution can be best represented in terms of the various Schechter parameters (e.g., [16, 28] vs. [13]).¹ Agreement between different determinations is generally good, when expressed in terms of the implied *UV* luminosity densities.

The *UV* LF appears to evolve with redshift in a reasonably smooth manner, with the characteristic magnitude M^* , the logarithm of the normalization ϕ^* , the faint-end slope α , and logarithm of the luminosity density all varying with redshift in an approximately linear manner from $z \sim 8$ to $z \sim 4$ [37, 24].

¹ This debate has continued for many years due to the significant degeneracies that exist between the different Schechter parameters (and also partially due to questions about whether the functional form of the LF is Schechter at $z \geq 7$: e.g., [35, 13]).

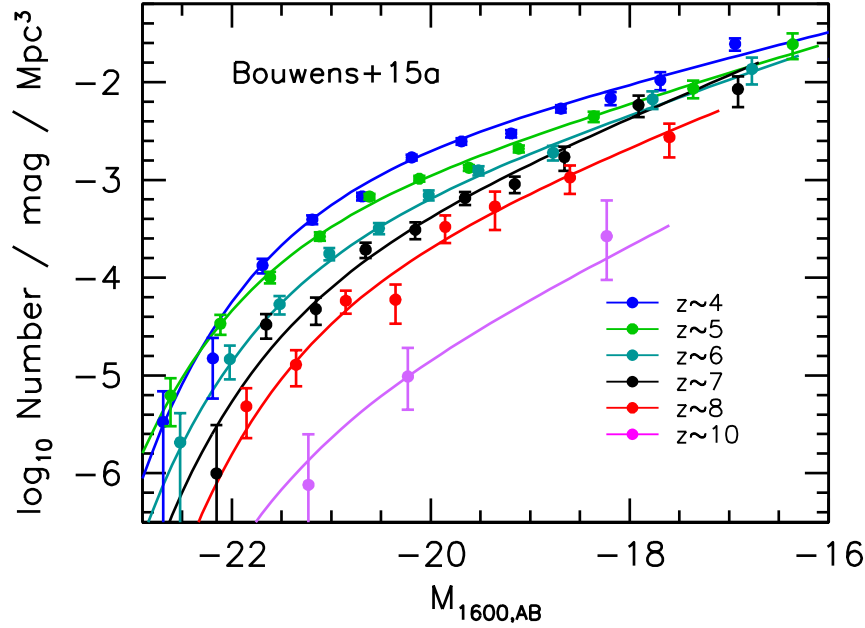


Fig. 1 Current state-of-the-art determinations of the *UV* luminosity functions at $z \sim 4$ (blue), $z \sim 5$ (green), $z \sim 6$ (cyan), $z \sim 7$ (red), $z \sim 8$ (black), and $z \sim 10$ (magenta) using the full data sets over the CANDELS + HUDF + HUDF-parallel + BoRG/HIPPIES fields [13] (§2.2). The solid circles represent stepwise maximum-likelihood determinations of the LFs while the solid lines are the Schechter function determinations. These luminosity functions allow for an accurate quantification of the luminosity density of galaxies in the rest-frame *UV* from $z = 4$ to $z = 10$ and therefore also an estimate of ionizing photons available to reionize the universe.

Here we provide one such fit to the evolution of the *UV* LF with redshift:

$$\begin{aligned}
 M_{UV}^* &= (-20.99 \pm 0.10) + (0.18 \pm 0.06)(z - 6) \\
 \phi^* &= (0.44^{+0.11}_{-0.10}) 10^{(-0.20 \pm 0.05)(z-6)} 10^{-3} \text{Mpc}^{-3} \\
 \alpha &= (-1.91 \pm 0.05) + (-0.13 \pm 0.03)(z - 6)
 \end{aligned}$$

The above fit makes full use of the likelihood contours derived by [13] for the galaxy LFs at $z \sim 5$ -8 and is illustrated in Figure 2. We have elected to make exclusive use of the constraints from [13] at $z = 5$, $z = 6$, $z = 7$, and $z = 8$ due to the relatively smooth increase in the characteristic luminosity L^* and normalization ϕ^* and flattening of the faint-end slope α observed over this redshift range (see also [36, 34]). These trends appear to be significant at $\geq 3\sigma$ in all three cases.

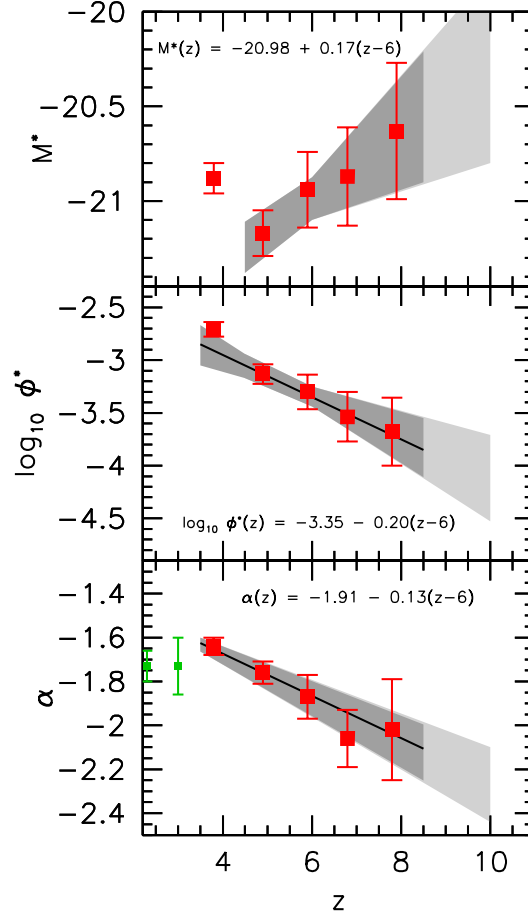


Fig. 2 Best-fit constraints on the evolution of the three Schechter parameters M^* (upper), ϕ^* (middle), and α (lower panels) to $z > 5$ using recent state-of-the-art luminosity function determinations from [13] (§2.2). The solid line is a fit of the $z \sim 4-8$ faint-end slope determinations to a line, with the 1σ errors (gray area: calculated by marginalizing over the likelihoods for all slopes and intercepts). Also shown are the faint-end slope determinations from [38] at $z \sim 2-3$ (green squares). The evolutionary trend most relevant for galaxies' reionizing the universe are the changes in the faint-end slope α . The best-fit trend with redshift (from $z \sim 5$ to $z \sim 8$) is $d\alpha/dz = -0.13 \pm 0.03$. Strong evidence (3.4σ) is found for a steepening of the UV LF from $z \sim 8$ to $z \sim 4$.

2.3 Faint-end Slope and Its Evolution

In deriving estimates of the total luminosity density ρ_{UV} in the largely unobservable population of ultra-faint galaxies, there are two considerations which are important. The first of these considerations is the faint-end slope α of the luminosity function – which gives the power-law relationship between the volume density of galaxies at some epoch and the UV luminosity of galaxies at that epoch. The second of these

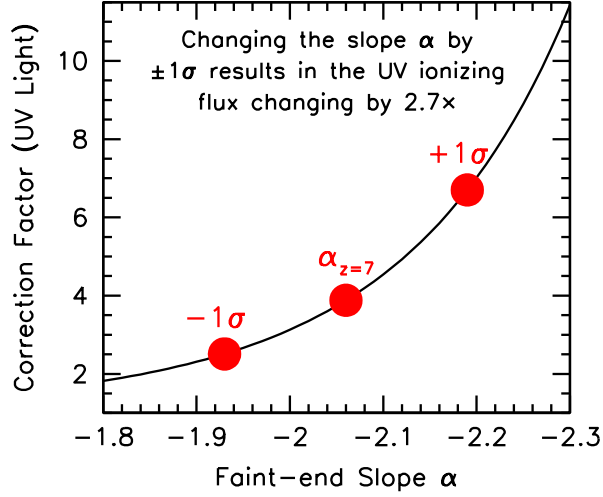


Fig. 3 The dependence of the integrated UV ionizing flux on the faint-end slope α (§2.3). The correction factors needed to convert the observed UV photon density to the total density for a given faint-end slope α (integrating to the expected theoretical cut-off in the LF at -10 mag) are shown for the current best estimate of the slope α at $z \sim 7$ and for the upper and lower $\pm 1\sigma$ limits of $\alpha \sim -1.93$ and $\alpha \sim -2.19$ [13]. The current uncertainties in the correction factor are large (the ratio between the upper and lower 1σ correction factors is a factor of ~ 3).

considerations is the minimum luminosity at which we would expect galaxies to efficiently form. We will discuss the first of these considerations in this subsection and discuss the second in §2.5.2.

To illustrate the importance of the faint-end slope α for estimates of the total luminosity density, we present in Figure 3 how the ratio of the total-to-observed luminosity density depends on the faint-end slope assumed. Even small uncertainties in the faint-end slope α can have a big impact on the inferred total luminosity density, as the faint-end slope α approaches a value of ~ -2 where the integral for the luminosity density (Eq. 1) formally becomes divergent.

The first accurate measurement of the faint-end slope α for galaxies in the high-redshift universe were performed by [39] at $z \sim 3$ in 1999. A relatively steep slope of ~ -1.6 was found, which implied that the surface density of galaxies on the sky approximately doubled for every $\Delta m = 1$ increase in apparent magnitude. Such steep faint-end slopes imply that lower luminosity galaxies contribute significantly to the overall luminosity density of the universe.

Precise measurements of the faint-end slope α at other redshifts ($z \sim 1-5$) took somewhat longer to become a reality. Most studies found faint-end slopes ranging from ~ -1.5 to ~ -1.7 [40, 26, 38, 41]. At higher redshifts, determinations of the faint-end slope were much less certain, but there was general agreement that the faint-end slope α was at least as steep at -1.7 [42, 26].

The first real progress in deriving the faint-end slope at $z \sim 7-8$ came with the availability of deep WFC3/IR data over the HUDF [24]. Combining constraints on

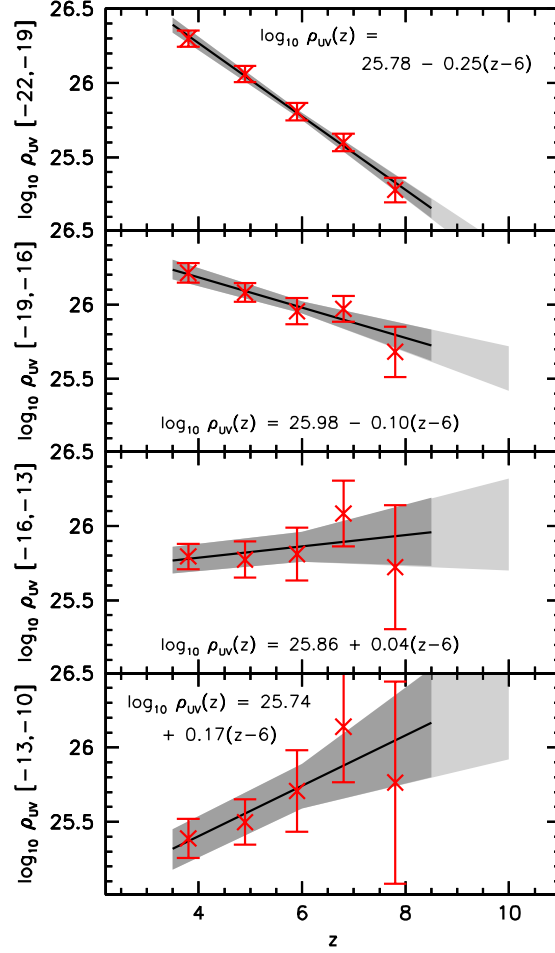


Fig. 4 The evolution of the UV luminosity density ρ_{UV} over various intervals in absolute magnitude, i.e., $-22 < M_{UV,AB} < -19$ (uppermost panel), $-19 < M_{UV} < -16$ (second uppermost panel), $-16 < M_{UV} < -13$ (second lowest panel), $-13 < M_{UV} < -10$ (lowest panel), based on the recent comprehensive determinations of the $z = 4-8$ LFs from [13] (§2.6). The red crosses and error bars give the determinations based on the LFs at specific redshifts, while the grey-shaded region gives the 68% confidence intervals assuming a linear dependence of $\log_{10} \rho_{UV}$ on redshift. Constraints on the evolution of this luminosity density over the magnitude range $-22 < M_{UV} < -16$ are largely based on the direct search results from Bouwens et al. [13] while the results over the magnitude range $-16 < M_{UV} < -10$ are based on extrapolations of the LF beyond what can be directly detected. If galaxy formation is particularly inefficient faintward of some luminosity, then we would expect that the luminosity densities derived here to be an overestimate.

the volume density of luminous $z \sim 7-8$ galaxies, with constraints on the volume density of significantly fainter galaxies from the new 192-orbit HUDF09 data set, [24] presented the first tantalizing evidence for a further steepening of the LF at

$z > 6$. A faint-end slope α of -2.01 ± 0.21 was found at $z \sim 7$ and -1.91 ± 0.34 at $z \sim 8$.

Towards the end of 2012, even deeper observations were obtained over the HUDF as a result of the HUDF12 campaign [25], extending the depth in the $1.1\mu\text{m}$ Y_{105} -band data by ~ 0.7 mag and adding observations at $1.4\mu\text{m}$ in the JH_{140} band. These new observations strengthened existing evidence at $z \sim 7$ and $z \sim 8$ that the faint-end slope at $z \sim 7-8$ was steep [28, 27]

The first definitive clarification of the evolution came with the UV LF determinations from [13]. In that study, LFs were derived from large $z \sim 4, 5, 6, 7, 8$, and 10 samples identified from the ~ 1000 arcmin² CANDELS + HUDF + HUDF-parallel + BoRG/HIPPIES data set [43, 44] and possible evolution in Schechter parameters considered. The faint-end slopes derived at high redshifts, i.e., $z \sim 7$ and $z \sim 8$, were much steeper ($\Delta\alpha \sim 0.4$) than those found at the low end of the redshift range considered by [13] (3.4σ significance). This is illustrated in the lowest panel of Figure 2. The advantage of mapping out the evolution of the LF over such a wide range in redshift using the same techniques and observational data is that it largely guarantees the results will be free of systematic errors.

The much steeper faint-end slopes to the UV LFs at early times has one particularly important implication. Lower-luminosity galaxies will evolve much less in their overall volume density with cosmic time than more luminous galaxies, and consequently still be very abundant in the early universe (Figure 4). As a result, such galaxies are expected to contribute the vast majority of the photons that reionize the universe.

2.4 Estimating the Production Rate of Lyman-Continuum Photons

To determine if the observed galaxy population can be successful in reionizing the universe, we must convert the overall luminosity density ρ_{UV} in the UV -continuum (~ 1600 Å) to the equivalent luminosity density in Lyman-continuum photons (≤ 912 Å). As this involves an extrapolation of the observed UV light to bluer wavelengths, one might expect the observed UV colors to provide us with the necessary information to perform this extrapolation more accurately.

It is conventional to model the spectrum of galaxies in the rest-frame UV as a power-law such that $f_\lambda \propto \lambda^\beta$ (or equivalently $f_\nu \propto \nu^{-(\beta+2)}$) where β is the UV -continuum slope and λ is the wavelength. While the spectrum of star-forming galaxies in the UV continuum cannot be perfectly described using a power-law parameterization, such a parameterization generally works for most of the spectral range to within $\pm 20\%$.

Over the last few years, significant effort has been devoted to quantifying the UV -continuum slope β distribution of galaxies as a function of both the UV luminosity and redshift of galaxies [48, 49, 50, 51, 46, 45, 52, 53, 54, 55, 47].

In general, the UV -continuum slopes β of galaxies at $z \sim 4-8$ have been found to have a mean β of ~ -1.6 at high luminosities and slowly trend towards bluer β 's

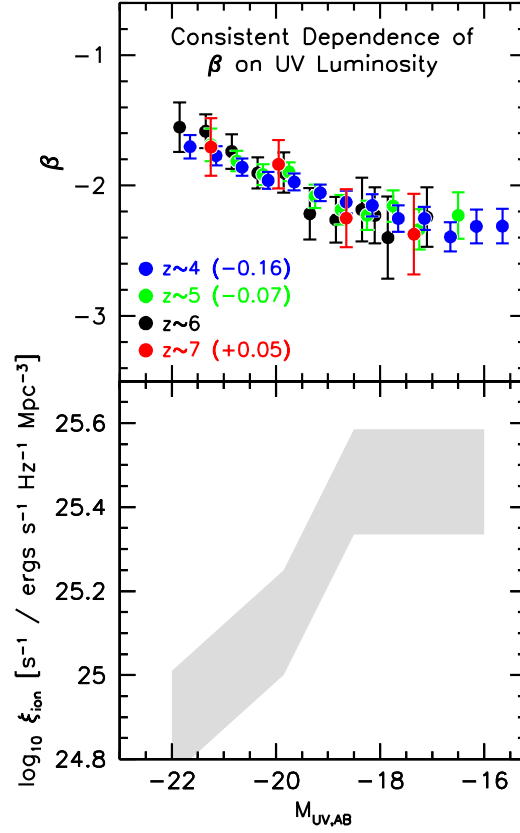


Fig. 5 (*upper*) Mean UV -continuum slope β of star-forming galaxies at $z \sim 4$ (blue), $z \sim 5$ (green), $z \sim 6$ (black), and $z \sim 7$ (red) versus their measured UV luminosities, as derived by [45] (§2.4). The mean β 's presented here are offset slightly depending on the redshift to illustrate the similarity of β vs. M_{UV} relations for galaxies in all four redshift intervals. The UV -continuum slope β exhibits a much stronger dependence on luminosity for galaxies brightward of -19 mag than it does faintward of this luminosity. A number of other recent studies [46, 47] have recovered a very similar dependence of β on UV luminosity, as shown here. (*lower*) Suggested conversion factors ξ_{ion} to use in transforming the observed luminosity density in the UV continuum to the equivalent density in ionizing photons. The preferred conversion factor can be estimated based on the mean UV -continuum slopes β derived for Lyman-break galaxies at a given redshift and luminosity (see Figure 7). The conversion factors suggested here are derived from mean β 's presented in the upper panel.

of ~ -2.2 at the lowest luminosities [46, 45, 47]. The relationship is remarkably similar for galaxies at $z \sim 4$, $z \sim 5$, $z \sim 6$, and $z \sim 7$, as illustrated in Figure 5.

There is some evidence for a weak evolution ($d\beta/dz \sim -0.10 \pm 0.05$) in β with redshift for lower luminosity galaxies, from $\beta \sim -2.3$ for $z \sim 7-8$ galaxies to $\beta \sim -2.1$ for $z \sim 4$ galaxies [46, 45, 55, 56, 57] (see Figure 5 and 8). The observed

evolution is consistent with that expected for the zero-attenuation UV slopes from simulations [58] (see also [59]). The scatter in the UV -continuum slopes is ~ 0.35 for the most luminous galaxies [51, 46, 53], but appears to decrease to ~ 0.15 for the lowest-luminosity galaxies [47].

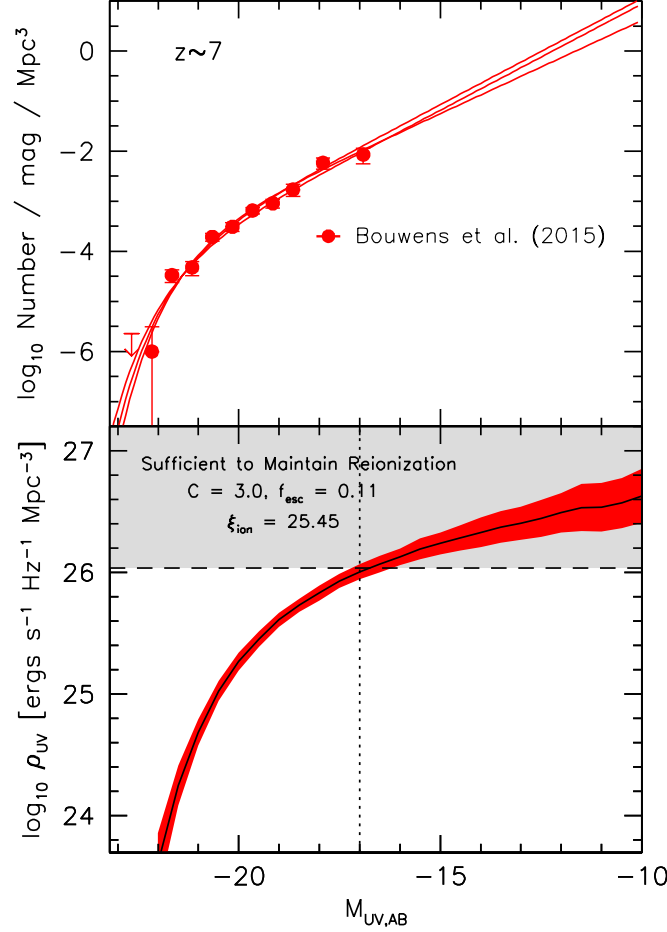


Fig. 6 (*top*) Best-fit constraints on the galaxy luminosity function at $z \sim 7$ in the rest-frame ultraviolet from [13] using observations from the full CANDELS, HUDF, and HUDF parallel programs (§2.2). Shown are both binned and parameterized constraints on the luminosity function, with uncertainties in the extrapolated relation represented by the different lines. (*bottom*) Maximum likelihood constraints (*black line*) on the UV luminosity density ρ_{UV} integrated to different lower luminosity limits presented relative to the requisite luminosity density in the UV needed to reionize the universe. The luminosity densities preferred at 68% confidence [13] are indicated with the red-shaded regions.

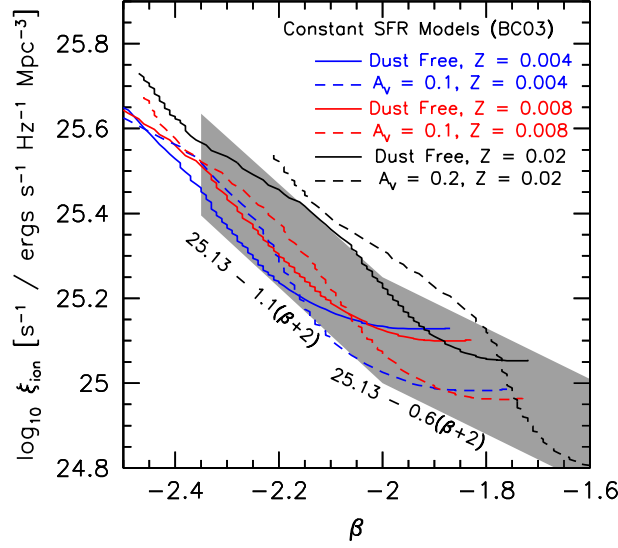


Fig. 7 A determination of how the production efficiency ξ_{ion} of Lyman-continuum photons per unit UV luminosity at 1600Å depends on the UV -continuum slope β (§2.4). These efficiencies are calculated from the Bruzual & Charlot [60] spectral synthesis library assuming a constant star formation rate adopting three different metallicities ($0.004Z_{\odot}$, $0.008Z_{\odot}$, and $0.02Z_{\odot}$) and a wide range in ages (ranging from an essentially instantaneous burst [10^5 years] to a stellar population of similar age to the universe itself [10^{10} years]). Both the case of no dust content and $\tau_V = 0.1/0.2$ [61] is considered, as indicated on the figure. β is computed over the spectral range 1700Å to 2200Å. The shaded envelopes indicate the approximate dependence of ξ_{ion} on β .

Since essentially all of the UV light produced by galaxies in the $z \sim 6-8$ universe derives from galaxies at very low luminosities (Figure 6), it is reasonable to use the β 's measured for lower luminosity galaxies to convert the luminosity densities in the UV continuum into the equivalent density of ionizing photons. The conversion factor can be estimated using the spectral synthesis models of [60], assuming a constant star-formation history and a variety of different ages and metallicities for the stars, as well as a modest amount of dust content. The conversion factors and β 's computed for many different model spectra are presented in Figure 7. Estimates of these conversion factors were previously estimated by [62] using earlier measurements of β for $z \sim 7$ galaxies [63].

Significantly enough, for the faint population of star-forming galaxies at $z \sim 5-8$, the mean UV -continuum slope β imply that the conversion factor to the ionizing luminosity density ξ_{ion} is approximately equal to $10^{25.45} s^{-1} / (ergs s^{-1} Hz^{-1})$. This is somewhat higher than the $10^{25.3} s^{-1} / (ergs s^{-1} Hz^{-1})$ conversion factor adopted by [16] and [64] and the $10^{25.2} s^{-1} / (ergs s^{-1} Hz^{-1})$ conversion factor adopted by [65] and [62].

2.5 Key Uncertainties in Computing the Ionizing Photon Density Contributed by Galaxies

2.5.1 Lyman-Continuum Escape Fraction

For $z > 6$ galaxies to have been successful in reionizing the universe, a modest fraction of the ionizing radiation emitted from their hot stars, i.e., $\geq 10\%$, must escape into the intergalactic medium. This general expectation has significantly motivated the search for such escaping radiation both at intermediate redshifts and in the nearby universe. Direct searches for such radiation from $z > 6$ galaxies, themselves, would also be interesting and provide the most relevant information on this issue, but are not really feasible, in that any escaping radiation from $z > 6$ galaxies would need to successfully redshift through the thick Lyman-series forest to allow for detection.

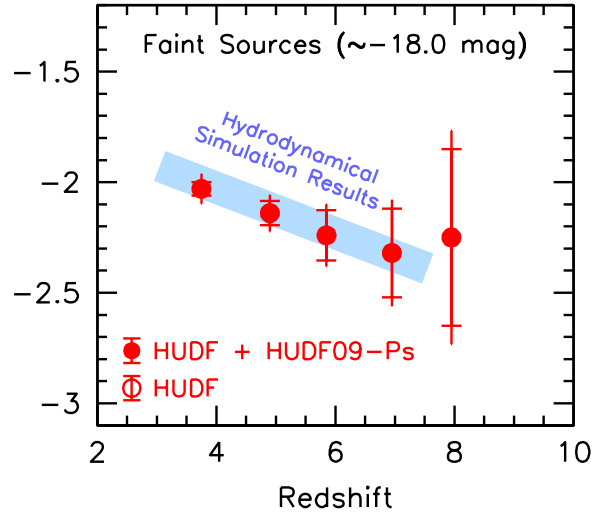


Fig. 8 The biweight mean UV -continuum slopes β observed by [45] for faint ($-19 \leq M_{UV,AB} \leq -17$) $z \sim 4$, $z \sim 5$, $z \sim 6$, $z \sim 7$, and $z \sim 8$ galaxies in the HUDF and HUDF-parallel fields (red solid circles: §2.4). 1σ uncertainties on each of the determinations are also shown, for the statistical uncertainties alone (including hashes at the ends) and including the systematic uncertainties (not including hashes). The expectations from hydrodynamical simulations [59] are shown for comparison with the thick light-blue line. The weak evolution observed in β is expected to result in $\sim 50 \pm 25\%$ more ionizing radiation for faint galaxies at $z \sim 7-8$ than at $z \sim 4$.

Remarkably enough, searches for leaking ionizing radiation from galaxies in the nearby universe has been largely a frustrating activity, with little success. Most such studies only result in ever more stringent upper limits on the ionizing radiation escaping from galaxies [66, 67, 68, 69, 70, 71, 72, 73]. Perhaps the most promising re-

sults in searches for escaping radiation from galaxies have come from the very compact star-forming galaxies, with a particularly dominant central component, where galaxies show evidence for having a low covering fraction of neutral hydrogen gas [74] and where one galaxy shows direct evidence for $\sim 20\%$ of the ionizing radiation escaping from the galaxy.

Efforts to identify significant leaks of ionizing radiation from $z \sim 2-3$ galaxies have been seemingly more successful than at $z \sim 0-1$. Though there is significant debate in the literature regarding the precise value of the escape fraction f_{esc} , the reported values for the escape fraction range from values of 2-5% [75] to 10-30% [76, 28, 77, 78].

The substantial scatter in estimated values for the escape fraction is a direct consequence of the challenges inherent in accurately quantifying it. A precise determination of this fraction requires accurate redshift measurements for a representative sample of intermediate-redshift sources, as well as a measurement of the flux blueward of the Lyman break. One issue of particular importance is that of foreground sources at lower redshift lying almost directly in front of star-forming galaxies and therefore effectively mimicking the signature of Lyman-continuum emission [e.g., 79, 75]. Another issue regards the possible exclusion of those sources showing the strongest Lyman-continuum emission from high-redshift samples [77]. Both issues continue to be the subject of debate in the literature [78].

Some discussion about how the escape fraction is defined is required, as it can be described in a variety of ways in the literature. Throughout most of the present chapter and in most self-consistent reionization models of the universe, the escape fraction f_{esc} discussed is the so-called “relative escape fraction” $f_{esc,rel}$ [80, 73]:

$$f_{esc,rel} = \frac{f_{esc}^{LyC}}{f_{esc}^{UV}} = \frac{(L_{UV}/L_{LyC})_{intr}}{(F_{UV}/F_{LyC})_{corr}} \quad (2)$$

where f_{esc}^{LyC} and f_{esc}^{UV} describes the fraction of Lyman Continuum and UV continuum photons, respectively, emitted from stars that successfully escape a galaxy into the IGM, where L_{UV} and L_{LyC} describe the intrinsic luminosities of galaxies in the UV -continuum and Lyman-continuum, respectively, prior to absorption by gas or dust, and where F_{UV} and F_{LyC} describe the measured fluxes of galaxies at UV continuum and Lyman-continuum wavelengths, after correction for IGM absorption.

Current observational estimates of the escape fraction at $z \sim 2-3$ are substantially higher than has been measured at lower redshift, strongly pointing towards the evolution in this escape fraction with cosmic time from higher fractions at intermediate-to-high redshift to very low fractions at $z \sim 0-1$ [73]. The apparent evolution strongly correlates with the evolution apparent in the escape fraction of $Ly\alpha$ photons [81] and the H I covering factor, as inferred from UV absorption lines [82]. Evolution in the escape fraction had also been speculated to help match the Thomson optical depths measured from the WMAP observations [83, 64].

In addition to the direct constraints on the escape fraction from a measurement of the Lyman-continuum fluxes for distant galaxies, there are several other promising ways of constraining it. One method makes use of the constraints on the density

of ionizing photons from studies of the Ly α forest. By modeling the observations of the Ly α forest, one can quantify the photoionization rate $\Gamma(z)$ and the mean free path for UV photons λ_{mfp} . Then, using the proportionality $\Gamma(z) \propto \epsilon \lambda_{mfp}$ and comparing this emissivity with the luminosity density in the UV continuum, one can obtain an average constraint on the escape fraction of the total galaxy population. The precise value of the escape fraction one infers depends somewhat on how faint one assumes that galaxy LF extends. Using this technique, [64] infer an escape fraction of $\sim 4\%$ at $z \sim 4$ based on the published photo-ionization rates $\Gamma(z)$ and mean free paths from [84] and [85] and the published LF results of [26] integrated to -10 AB mag. Assuming a minimal escape of Lyman-continuum photons from most luminous galaxies ($M_{UV,AB} < -19$), the implied escape fraction would be $\sim 10\%$.

Alternate constraints on the escape fraction of galaxies come from the study of Gamma Ray Bursts [86] in $z \sim 2-4$ galaxies. Gamma-ray bursts are potentially ideal for constraining the Lyman-continuum escape fraction, if these bursts show a similar spatial distribution in star-forming galaxies as the hot stars producing ionizing photons. The presence or absence of one optical depth of neutral hydrogen absorption can be immediately seen from optical follow-up spectroscopy of the bursts. Of the 28 GRB systems examined by [86] where the underlying column density of atomic hydrogen has been measured, only 1 shows a relative absence of neutral hydrogen in front of the burst, resulting in f_{esc}^{LyC} fraction estimate of $2 \pm 2\%$ (implying a $f_{esc} = 0.04 \pm 0.04$ assuming $f_{esc}^{UV} \sim 0.5$ based on the measured values of the UV -continuum slope β for faint galaxies and a Calzetti et al. [87] extinction law).

Direct studies of Lyman-continuum emission from $z \sim 2-3$ galaxies provide some evidence for galaxies at lower luminosities or with Ly α emission having $\sim 2-4\times$ higher values of the escape fraction than for the highest luminosity galaxies [76, 28]. If true, evolution in the density of ionizing UV radiation would much more closely follow the evolution in the luminosity density of faint ($M_{UV,AB} < -19$) galaxies. Given the minimal evolution in the luminosity density of the faintest sources (lowest two panels of Figure 4), one might expect a similarly slow evolution in the density of ionizing radiation with cosmic time. Indeed, a model with a nearly constant escape fraction of $\sim 10\%$ for lower luminosity ($M_{UV,AB} > -19$) galaxies would succeed in matching essentially all observational constraints on the Lyman-continuum escape fraction discussed here.

2.5.2 Faint End Cut-off to LF

If the faint-end slope α of the UV LF is close to -2 , then one could potentially expect a particularly significant contribution of galaxies at arbitrarily faint luminosities to the reionization of the universe. A faint-end slope of -2 is sufficiently steep for the total luminosity density to be technically divergent if the integral (Eq. 1) is extended all the way to zero.

In reality, however, the galaxy LF cannot extend to arbitrarily low luminosities with such a steep faint-end slope and must eventually turn over at some luminosity. This is due to the challenge especially low-mass collapsed halos have in accreting

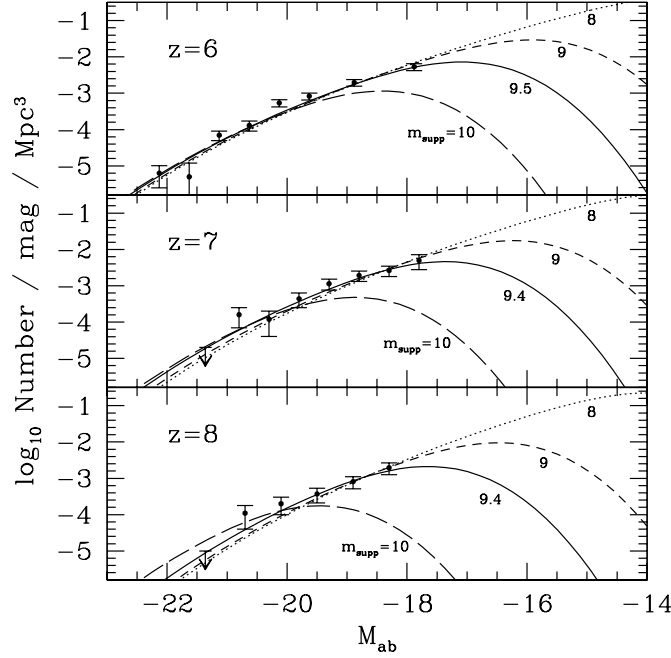


Fig. 9 An illustration of several model luminosity functions [88] with a cut-off at the faint end (§2.5.2). Results are shown relative to the LFs observed at $z \sim 6$ (top), $z \sim 7$ (middle), and $z \sim 8$ (lowest) panel. Dotted, short-dashed, and long-dashed curves are LFs assuming $m_{\text{supp}} = 8, 9$, and 10 , respectively, with the best-fit value of L_{10} for each value of m_{supp} . The solid lines show results with the absolute minimum value of chi-square at each redshift. The best-fit values of m_{supp} are $9.47, 9.4$, and 9.42 , for $z = 6, 7$, and 8 , respectively.

or retaining significant amounts of cool gas necessary for star formation. There are many compelling physical reasons to expect galaxies to only efficiently form in halos above a certain mass [92, 88]. Inefficient gas cooling [93], supernovae winds [94], and a high UV background [95] are all issues that are likely to contribute to suppressing significant star formation in very low-mass ($< 10^8 M_{\odot}$) halos. Determining at which luminosity the *UV* LF cuts off is clearly important for assessing the total reservoir of ionizing radiation available to reionize the universe (e.g., see Figure 9).

Ascertaining to which luminosity the *UV* LF extends observationally is clearly quite challenging and will likely remain challenging for the foreseeable future. Searches for faint $z \sim 2$ galaxies find an abundance of galaxies to -14 mag [89] and provide no indication for an abrupt cut-off (see Figure 10). Simple reconstructions of the faint-end of the *UV* LF using the star-formation histories of dwarf galaxies in the local group similarly suggest that the *UV* LF extends down to at least -14 mag and potentially down to -5 mag [96] (suggestively similar to that found in the very high-resolution simulations of [97]).

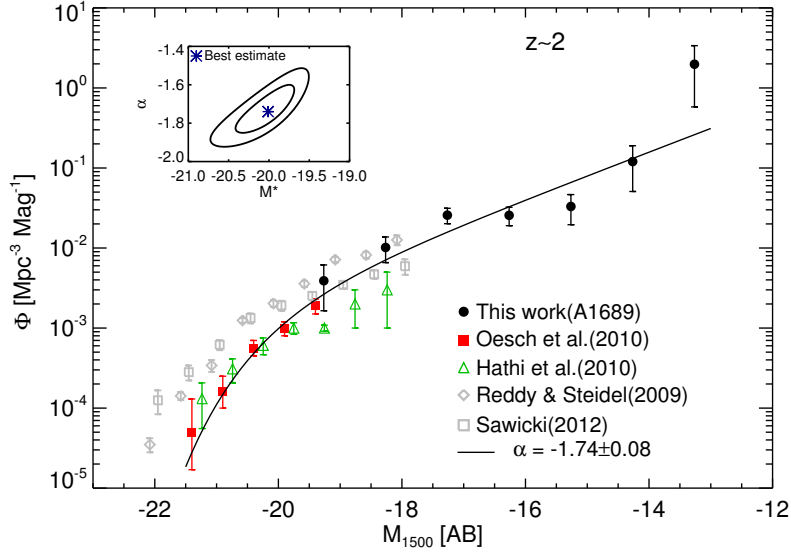


Fig. 10 The estimated UV luminosity function at $z \sim 2$ derived by [89] using highly-magnified, gravitationally-lensed galaxies behind Abell 1689 (*solid black circles*). Also shown are the volume densities of more luminous galaxies at $z \sim 2$ from wider-area probes (*assorted points*: [90, 38, 41, 91]). The solid line shows the $z \sim 2$ LF derived by a combined fit to the fainter sources discovered behind Abell 1689 and more luminous sources found from wide-area searches. The volume density of faint sources discovered behind Abell 1689 appears consistent with what is found over wide-area surveys at -19 mag, but extends to -14 mag with a power-law-like slope. This suggests that such faint galaxies plausibly exist at $z \sim 6-10$ and can potentially reionize the universe (§2.5.2).

While one could potentially hope to observe the faintest galaxies with gravitational lensing or with JWST, such techniques and advances in technology only allow us to gain a factor of 10 in sensitivity over what is state of the art at present (i.e., allowing to view galaxies without the aid of lensing to ~ -16 mag [~ -14 with lensing]). If the faint end of the LF extends faintward of -13 , it is unlikely that direct probes will be successful in revealing where the UV LF ultimately cuts off.

2.5.3 Evolution of the UV LF at $z > 8$

For galaxies at the highest redshifts $z > 8$, there is much more uncertainty regarding how the UV LF evolves with cosmic time. Most early results on the volume density of $z \sim 9-10$ galaxies [98, 99, 100, 25] suggested that the luminosity density of galaxies at $z \sim 9-10$ might be significantly less than what one would derive extrapolating the $z \sim 4-8$ results to $z \sim 10$.

This suggested that galaxies might exhibit a slightly more rapid evolution with time at $z > 8$ than they exhibited over the redshift interval $z = 4-8$. The rationale for the more rapid evolution observed was unclear, but was thought to potentially arise

from the halo mass function evolution not translating into a smooth evolution of the UV LF with redshift. As [100] demonstrate, results from a number of independent theoretical models [101, 102, 59, 103, 104] predict a slightly more rapid change in the luminosity density evolution at $z > 8$ than from $z = 8$ to $z = 4$ (but see however the results of the Behroozi et al. [105] model). Of course, another explanation for the trend could be one of dust extinction, as the early $z = 9$ -10 results show better continuity with the $z = 4$ -8 results, if considered after dust correction. This idea was implicitly first noted by [106], but has also been discussed in later work [13, 34].

Deeper searches over the Hubble Deep Field and parallel fields [25, 100] yielded a slight deficit in the luminosity density similar to those initially obtained by [98] and [99]. Similarly, searches for $z = 9$ -11 galaxies over lensing clusters also suggested a slight deficit at $z \sim 9$ relative to lower-redshift trends ([107]; but see also [108]). However, the $z \sim 11$ search results of Coe et al. [109] suggested no change in the ρ_{UV} trends to $z \sim 11$.

More recently, however, new $z \sim 9$ and $z \sim 10$ search results [110, 111, 112] from the Frontier Fields program [113] show somewhat higher volume densities than what was initially found over the Hubble Ultra Deep Field and deep parallel fields. At face value, this suggests that $z \sim 9$ -10 galaxies might have been underdense over the Chandra Deep Field South, and the true average density at $z \sim 9$ -10 is higher and also consistent with an extrapolation from lower redshift. However, the Hubble Frontier Fields program is still ongoing, and it is not yet clear whether the evolution in UV LF at $z > 8$ is essentially a continuation of the evolution from $z \sim 8$ to $z \sim 4$ or some acceleration is present.

2.6 The Ionizing Photon Density Produced by Galaxies

Using a similar procedure to many previous analyses [65, 64, 62], we can put together current constraints on the evolution of the UV luminosity function with an empirically-calibrated model for the production and release of ionizing radiation from $z > 6$ galaxies. Following [62], we parameterize the total density of ionizing photons $\dot{N}_{ion}(z)$ as

$$\dot{N}_{ion}(z) = \rho_{UV}(z) \xi_{ion} f_{esc} \quad (3)$$

where $\rho_{UV}(z)$ represents the rest-frame UV luminosity density, ξ_{ion} represents the conversion factor from UV luminosity to ionizing radiation, and f_{esc} indicates the fraction of ionizing radiation that escapes from galaxies after modulation by dust and neutral hydrogen within galaxies.

In computing the cosmic ionizing emissivity $\dot{N}_{ion}(z)$ from the UV luminosity density $\rho_{UV}(z)$, we take $\xi_{ion} = 10^{25.45} \text{ s}^{-1} / (\text{ergs s}^{-1} \text{ Hz}^{-1})$, consistent with lower luminosity galaxies dominating the UV luminosity density at $z > 4$ and faint galaxies having a UV -continuum slope β of -2.2 (§2.4). The escape fraction f_{esc} is chosen so that the universe finishes reionization at $z \sim 6$, consistent with observations, and so that the Thomson optical depth matches that seen in the observations. While

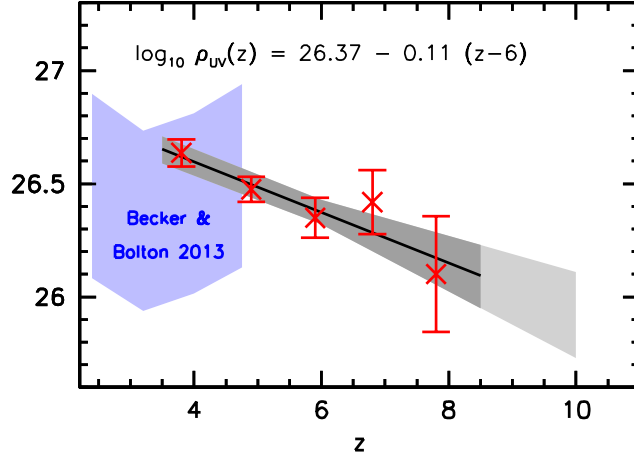


Fig. 11 The evolution of the UV luminosity density over a larger range in absolute magnitude than considered in Figure 4, i.e., $-23 < M_{UV,AB} < -13$, based on the recent comprehensive determinations of the $z = 4-8$ LFs from [13] (§2.6). The points and shaded regions are as in Figure 4 and similar caveats apply. Also shown on the right axis of this figure is the equivalent cosmic ionizing emissivity that galaxies over the specified luminosity range produce for the conversion factor $\log_{10} f_{esc} \xi_{ion} = 24.53 \text{ s}^{-1}/(\text{ergs s}^{-1} \text{Hz}^{-1})$. One recent measurement of the cosmic ionizing emissivity at $z \sim 2-4.75$ from [114] is also shown for context (*light-blue-shaded area*: 68% confidence region).

it is not possible to motivate the value 0.11 for the escape fraction purely based on observational considerations, the chosen value does fall within the allowed range.

The estimated ionizing emissivity from our fiducial model is presented in Figure 11. As should be clear by our procedure for choosing f_{esc} , the overall emissivity estimated here is highly uncertain. The three factors that contribute to the overall estimate could be plausibly different by 0.2 dex (ξ_{ion}), 0.8 dex (f_{esc}), and 0.4 dex (ρ_{UV}) from the baseline model presented here. While f_{esc} is plausibly known to better than 0.3 dex at $z \sim 3$ for L^* and sub- L^* galaxies, it is completely unclear what f_{esc} is for ultra-faint galaxies at $z \sim 6-10$. Uncertainties in ρ_{UV} result from a lack of knowledge regarding where the truncation of the UV LF occurs.

Also shown on this same figure are constraints on the ionizing emissivity from observations of the $\text{Ly}\alpha$ forest [114] at $z \sim 2-4.75$ (see [64] for earlier constraints on this emissivity). It is clear that the emissivity produced by the present model is overall in excellent agreement with the observational constraints. One potential resolution to the slight tension between the ionizing emissivity presented here and observational constraints at $z \sim 4$ is by accounting for the fact that a significant fraction of the luminosity density at $z \sim 4$ derives from particularly luminous galaxies and those galaxies seem to show a lower escape fraction [76, 115]. The ionizing emissivity produced by the present model is also in reasonable agreement with other models in the literature [e.g. 62, 116].

3 Self-Consistent Models of Reionization

3.1 Standard Reionization Model Using Galaxies

To determine the impact of the ionizing photon production from galaxies on the ionization state of atomic hydrogen at $z \geq 5$, it is conventional to follow the evolution of this ionization state with cosmic time. The simplest way to do this is by lumping the ionized hydrogen in the $z > 6$ IGM into a single quantity Q_{HII} , the filling factor of ionized hydrogen, and modeling its evolution with cosmic time with the following differential equation [65]:

$$\frac{dQ_{HII}}{dt} = \frac{-Q_{HII}}{\langle t_{rec} \rangle} + \frac{\dot{N}_{ion}(z)}{n_H(0)} \quad (4)$$

where $\dot{N}_{ion}(z)$ is the ionizing emissivity produced by the observed population of galaxies, n_H corresponds to the comoving volume density of neutral hydrogen in the universe and $\langle t_{rec} \rangle$ corresponds to the recombination time for neutral hydrogen

$$\langle t_{rec} \rangle = 0.88 \text{Gyr} \left(\frac{1+z}{7} \right)^{-3} \left(\frac{T_0}{2 \times 10^4 \text{K}} \right)^{-0.7} (C_{HII}/3)^{-1} \quad (5)$$

where C_{HII} is the clumping factor of neutral hydrogen ($\langle n_{HII}^2 \rangle / \langle n_{HII} \rangle^2$) and T_0 is the IGM temperature at mean density. The temperature T_0 is taken to be 2×10^4 K to account for the heating of the IGM due to the reionization process itself [117]. The above expression for the recombination time t_{rec} has been updated from the expression given in [64] to reflect the new results from Planck [5], where $H_0 = 67.51 \pm 0.64$, $\Omega_\Lambda = 0.6879 \pm 0.0087$, $\Omega_m = 0.3121 \pm 0.0087$, $\Omega_b h^2 = 0.02230 \pm 0.00014$, and $\tau = 0.066 \pm 0.016$. We develop a similar set of equations in Chapter XXX.

The whole exercise of self-consistently following the evolution of Q_{HII} is a valuable one. Importantly, it allows us to test whether the ionizing emissivity the observed galaxy population plausibly produces can self-consistently satisfy a variety of different constraints on the ionization state of the universe at $z \sim 6-10$. The most important of these constraints are the redshift at which reionization is complete, what the ionization state of the universe is at $z \sim 7-8$ where Ly α emitters and galaxies can be examined, and the Thomson optical depths τ measured from probes of the CMB.

There are many examples of similar analyses in the literature [e.g., 118, 119, 120, 83, 16, 64, 121, 62, 122, 123, 116]. Several of the first of these analyses to discuss many of the most important constraints discussed above include [119, 120, 83, 16, 64, 121]. Arguably the most sophisticated and well-developed of these include [83, 64, 62]. However, in appreciating the insight and value provided by such analyses, it is important to realize such analyses ignore one important effect: the most significant sinks for ionizing sources almost certainly lie in exactly

the same regions that produce the majority of the ionizing photons. As these regions are denser and therefore have higher recombination rates than the cosmic average, this effect would cause the process of reionization to occur slower than calculated for the simplistic models presented here [124].

Figure 12 shows how the filling factor of ionized hydrogen evolves with redshift using the estimate we provide in §2.6 of the ionizing radiation coming from galaxies (Figure 11) and adopting a clumping factor of $C_{HII} = 3$. The universe finishes reionization somewhere between $z = 5.5$ and $z = 6.5$ in the present model, depending upon whether one takes the ionizing emissivity to be at lower or upper end of the range presented in Figure 11. The calculated filling factor Q_{HII} is in plausible agreement with many of the prominent constraints shown in Figure 12. The Thomson optical depth derived from this fiducial model is also in excellent agreement with the new Thomson optical depth constraints from Planck $\tau = 0.066 \pm 0.016$ (Figure 13).

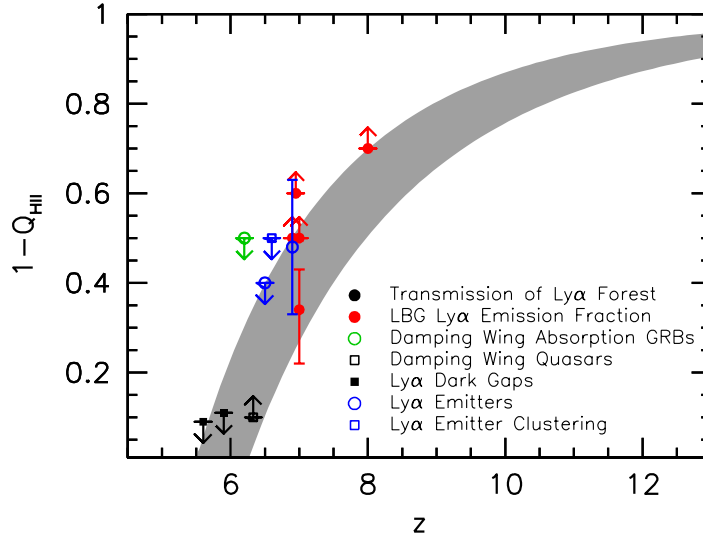


Fig. 12 Filling factor of neutral hydrogen ($1 - Q_{HII}$: the filling factor of ionized hydrogen) versus redshift based on the evolutionary model presented in §3.1 based on the LF results from [13], the optical depth results from citePL15, and many other assorted constraints on the reionization of the universe presented in this figure. See [62] and [116] for a detailed description of these constraints (§3.1).

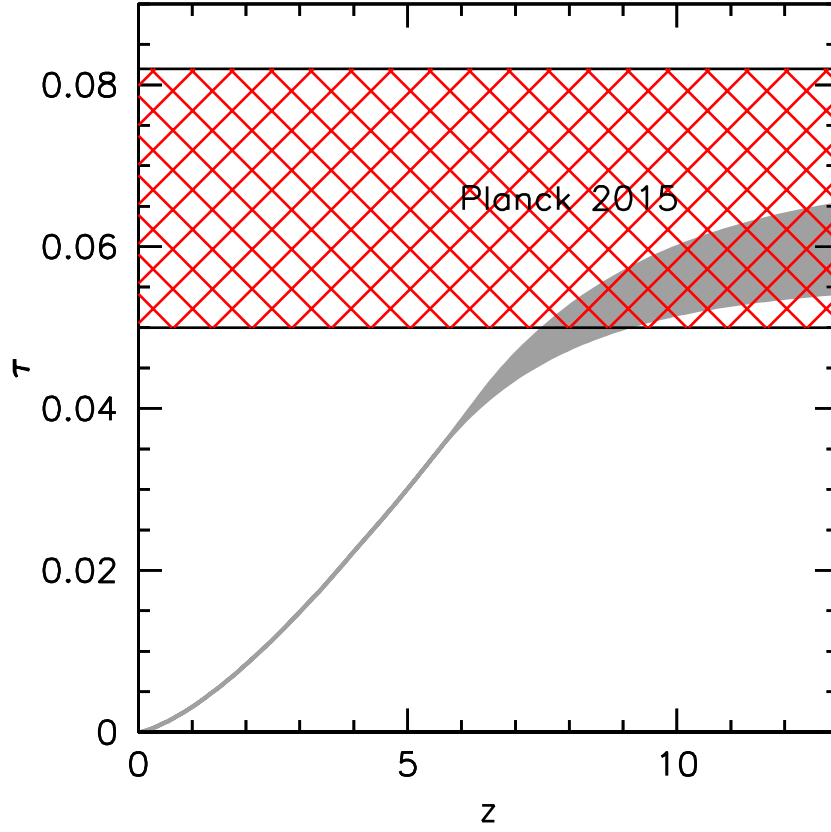


Fig. 13 Cumulative contribution of the ionized hydrogen and helium from $z = 0$ to an arbitrarily high redshift (*shaded grey contour*) from the model for the ionizing emissivity presented in Figure 11 and assuming a clumping factor C_{HII} of 3 (§3.1). The Planck 3-year results are shown with the hatched redshift region $\tau = 0.066 \pm 0.016$.

3.2 Does the Inferred Evolution in the Cosmic Ionizing Emissivity Match that Expected From Galaxies?

As the analysis from the previous subsection illustrates, it is clear that one can create a self-consistent model for the reionization of the universe using the observed galaxy population as a basis.

While such demonstrations are encouraging, they do not really address the question of uniqueness and whether galaxies uniquely fit the profile of those sources needed to provide the bulk of the photons for reionizing the universe. This is an

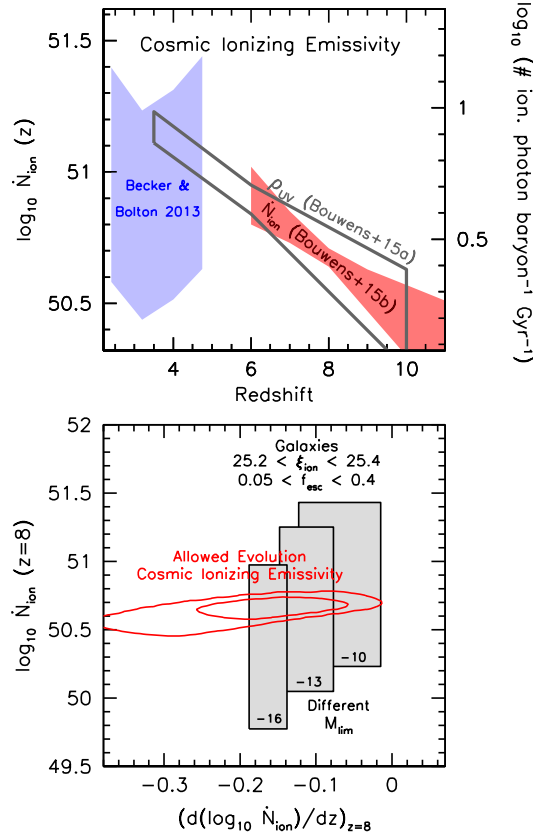


Fig. 14 (*upper*) The evolution of the cosmic ionizing emissivity inferred by [125] (*shaded red region*) using several of the most prominent observational constraints on the ionization state of the universe [2, 126, 5] (see §3.2). The vertical axis on the right-hand side gives the equivalent number of ionizing photons produced per Gyr per baryon in the universe. The light-blue-shaded region is the emissivity at $z \sim 2-4.75$ derived by [114]. The region demarcated by the thick grey lines shows the evolution of the *UV* luminosity density, converted to an emissivity using a constant conversion factor $\log_{10} f_{esc} \xi_{ion} = 24.53 \text{ s}^{-1}/(\text{ergs s}^{-1} \text{ Hz}^{-1})$. The evolution inferred for the cosmic ionizing emissivity at $z > 6$, i.e., $(d \log_{10} \dot{N}_{ion}(z)/dz)_{z=8} = -0.15^{+0.09}_{-0.11}$, is similar to the observed evolution in the *UV* luminosity density for galaxies derived by [13], i.e., $\log_{10} \rho_{UV} = -0.11 \pm 0.04$. While one could consider using a slightly different set of constraints than what [125] consider to derive the evolution of the cosmic ionizing emissivity, this result does suggest that galaxies do indeed drive the reionization of the universe. (*lower*) 68% and 95% likelihood contours on $\log_{10} \dot{N}_{ion}(z=8)$ and $(d \log_{10} \dot{N}_{ion}/dz)_{z=8}$ derived by [125] from the prominent observational constraints on the ionization state of the universe (§3.2). Shown with the grey squares are the equivalent parameters expected for galaxies based on the observations [13] for a range of f_{esc} 's and ξ_{ion} 's for three different faint-end cut-offs to the luminosity function M_{lim} (−10 mag, −13 mag, and −16 mag).

important topic, given the large uncertainties in the many factors that contribute to the calculation of the ionizing emissivity for galaxies.

To address the question of uniqueness, [125] made use of the some of the best constraints on the ionization state of the universe [e.g., 2, 126, 5] to try to infer the evolution of the cosmic ionizing emissivity $\dot{N}_{ion}(z)$ (see also [127]). In the results shown in Figure 14, [125] presented constraints on the evolution of the emissivity towards high redshift. In particular, $d(\log_{10} \dot{N}_{ion})/dz$ was found to be equal to $-0.15^{+0.09}_{-0.11}$ at $z = 8$. This is very similar to the observed evolution in the UV luminosity density of galaxies ρ_{UV} integrated to -13 , which have an equivalent logarithmic slope ($d\log_{10} \rho_{UV}/dz$) of -0.11 ± 0.04 at $z = 8$. The similar dependencies of the two quantities on redshift are illustrated in the top panel of Figure 14.

To take this comparison of the galaxy luminosity density with the required ionizing emissivity one step further, the lower panel of Figure 14 casts the comparison in terms of the required emissivity $\dot{N}_{ion}(z)$ at $z = 8$ and $(d(\log_{10} \dot{N}_{ion})/dz)_{z=8}$. Also presented in this panel are the expected parameters for the galaxy population assuming different escape fractions f_{esc} , different production rates of Lyman-continuum photons ξ_{ion} , different faint-end cut-offs to the LF.

It should be clear that one can produce the required ionizing emissivity with a wide variety of different parameter combinations (f_{esc} , ξ_{ion} , M_{lim}). Even though there are large observational uncertainties on each of the parameters in isolation, collectively they can be constrained quite well, using current constraints on the ionization state of the IGM at $z > 6$.²

4 Future Prospective

In both the present and immediate future, progress is being made with the Hubble Frontier Fields program [113]. This program is obtaining ultra-deep images of six different galaxy clusters with the Hubble and Spitzer Space Telescopes over a three-year period. The goal of this initiative is to obtain our deepest-ever views of the distant universe, by combining the power of extraordinarily deep exposures with Hubble and Spitzer with magnification boosts from gravitational lensing by the galaxy clusters. Accounting for the $\sim 5\times$ typical magnification factors expected from gravitational lensing over these fields, our view from this program will extend to sources fainter than even seen in the Hubble Ultra Deep Field [23, 24, 25, 128].

In total, 840 orbits of HST imaging observations are being obtained on these clusters, reaching to ~ 28.7 AB mag. Half of the observing time is being devoted to deep near-IR observations and half to deep optical observations over these fields. Spitzer has also invested 1000 hours of Director's Discretionary time observing these fields to depths of 26.3-26.8 mag (5σ) in the $3.6\mu\text{m}$ and $4.5\mu\text{m}$ bands, $\geq 3\times$ deeper than the observations over the CLASH clusters.

² For example, at present, it is not really known if the escape fraction f_{esc} of faint galaxies at $z \sim 7-8$ is 0.08 or 0.3 from the observations. Both possibilities could be accommodated within the uncertainties by making different assumptions about the faint-end cut-off to the LF M_{lim} or to the Lyman-continuum production efficiency ξ_{ion} .

Longer term, progress will come when the James Webb Space Telescope (JWST) begins operations in 2019. The NIRCAM instrument on the JWST will be $\sim 10\times$ as efficient as the HST WFC3/IR instrument in discovering $z \sim 7\text{--}10$ galaxies and will completely revolutionize the search for $z \geq 12$ galaxies with high sensitivities to $5\mu\text{m}$. Despite this dramatic leap in capabilities and a much improved knowledge of the total photon output of galaxies to specific lower luminosity limits, it seems unlikely that JWST will probe faint enough to quantify the volume density of the lowest luminosity sources at $z \sim 7\text{--}10$. Nevertheless, we remark that indirect detections of the emission from these galaxies may be possible in the not too distant future (see Chapter XXX). Whatever the success of such experiments, the impact of the lowest luminosity sources on the reionization of the universe seems likely to remain an open issue for many years into the future.

Acknowledgements Many thanks are due to my scientific collaborators Garth Illingworth, Pascal Oesch, and Ivo Labbe for some of the text and figures presented here, which were developed through discussions we had for proposals we wrote together. Significant thanks is also due to Michael Kuhlen, Claude Faucher-Giguère, and Brant Robertson who wrote recent manuscripts which served as a guide to writing this chapter. I also acknowledge support from NASA grant HST-GO-11563, ERC grant HIGHZ #227749, and a NWO vrij competitie grant 600.065.140.11N211

References

- [1] X. Fan, V. K. Narayanan, M. A. Strauss, R. L. White, R. H. Becker, L. Pentericci, and H.-W. Rix. Evolution of the Ionizing Background and the Epoch of Reionization from the Spectra of $z \sim 6$ Quasars. *AJ*, 123:1247–1257, March 2002.
- [2] X. Fan, M. A. Strauss, R. H. Becker, R. L. White, J. E. Gunn, G. R. Knapp, G. T. Richards, D. P. Schneider, J. Brinkmann, and M. Fukugita. Constraining the Evolution of the Ionizing Background and the Epoch of Reionization with $z \sim 6$ Quasars. II. A Sample of 19 Quasars. *AJ*, 132:117–136, July 2006.
- [3] G. Hinshaw, D. Larson, E. Komatsu, D. N. Spergel, C. L. Bennett, J. Dunkley, M. R. Nolta, M. Halpern, R. S. Hill, N. Odegard, L. Page, K. M. Smith, J. L. Weiland, B. Gold, N. Jarosik, A. Kogut, M. Limon, S. S. Meyer, G. S. Tucker, E. Wollack, and E. L. Wright. Nine-year Wilkinson Microwave Anisotropy Probe (WMAP) Observations: Cosmological Parameter Results. *ApJS*, 208:19, October 2013.
- [4] M. Ouchi, K. Shimasaku, H. Furusawa, T. Saito, M. Yoshida, M. Akiyama, Y. Ono, T. Yamada, K. Ota, N. Kashikawa, M. Iye, T. Kodama, S. Okamura, C. Simpson, and M. Yoshida. Statistics of 207 Ly α Emitters at a Redshift Near 7: Constraints on Reionization and Galaxy Formation Models. *ApJ*, 723:869–894, November 2010.
- [5] Planck Collaboration, P. A. R. Ade, N. Aghanim, M. Arnaud, M. Ashdown, J. Aumont, C. Baccigalupi, A. J. Banday, R. B. Barreiro, J. G. Bartlett, and

- et al. Planck 2015 results. XIII. Cosmological parameters. *ArXiv e-prints*, February 2015.
- [6] I. D. McGreer, A. Mesinger, and X. Fan. The first (nearly) model-independent constraint on the neutral hydrogen fraction at $z \sim 6$. *MNRAS*, 415:3237–3246, August 2011.
 - [7] I. D. McGreer, A. Mesinger, and V. D’Odorico. Model-independent evidence in favour of an end to reionization by $z \approx 6$. *MNRAS*, 447:499–505, February 2015.
 - [8] C. J. Willott, P. Delorme, C. Reyl  , L. Albert, J. Bergeron, D. Crampton, X. Delfosse, T. Forveille, J. B. Hutchings, R. J. McLure, A. Omont, and D. Schade. The Canada-France High- z Quasar Survey: Nine New Quasars and the Luminosity Function at Redshift 6. *AJ*, 139:906–918, March 2010.
 - [9] I. D. McGreer, L. Jiang, X. Fan, G. T. Richards, M. A. Strauss, N. P. Ross, M. White, Y. Shen, D. P. Schneider, A. D. Myers, W. N. Brandt, C. DeGraf, E. Glikman, J. Ge, and A. Streblyanska. The $z = 5$ Quasar Luminosity Function from SDSS Stripe 82. *ApJ*, 768:105, May 2013.
 - [10] M. Ricotti and J. P. Ostriker. X-ray pre-ionization powered by accretion on the first black holes - I. A model for the WMAP polarization measurement. *MNRAS*, 352:547–562, August 2004.
 - [11] P. Madau, M. J. Rees, M. Volonteri, F. Haardt, and S. P. Oh. Early Reionization by Miniquasars. *ApJ*, 604:484–494, April 2004.
 - [12] P. A. Oesch, R. J. Bouwens, G. D. Illingworth, I. Labb  , R. Smit, M. Franx, P. G. van Dokkum, I. Momcheva, M. L. N. Ashby, G. G. Fazio, J.-S. Huang, S. P. Willner, V. Gonzalez, D. Magee, M. Trenti, G. B. Brammer, R. E. Skelton, and L. R. Spitler. The Most Luminous $z \sim 9$ -10 Galaxy Candidates Yet Found: The Luminosity Function, Cosmic Star-formation Rate, and the First Mass Density Estimate at 500 Myr. *ApJ*, 786:108, May 2014.
 - [13] R. J. Bouwens, G. D. Illingworth, P. A. Oesch, M. Trenti, I. Labb  , L. Bradley, M. Carollo, P. G. van Dokkum, V. Gonzalez, B. Holwerda, M. Franx, L. Spitler, R. Smit, and D. Magee. UV Luminosity Functions at redshifts $z \sim 4$ to $z \sim 10$: 10000 Galaxies from HST Legacy Fields. *ApJ*, 803:34, 2015.
 - [14] R. F. Carswell, J. A. J. Whelan, M. G. Smith, A. Boksenberg, and D. Tytler. Observations of the spectra of Q0122-380 and Q1101-264. *MNRAS*, 198:91–110, January 1982.
 - [15] S. Bajtlik, R. C. Duncan, and J. P. Ostriker. Quasar ionization of Lyman-alpha clouds - The proximity effect, a probe of the ultraviolet background at high redshift. *ApJ*, 327:570–583, April 1988.
 - [16] R. J. Bouwens, G. D. Illingworth, P. A. Oesch, M. Trenti, I. Labb  , M. Franx, M. Stiavelli, C. M. Carollo, P. van Dokkum, and D. Magee. Lower-luminosity Galaxies Could Reionize the Universe: Very Steep Faint-end Slopes to the UV Luminosity Functions at $z \geq 5$ -8 from the HUDF09 WFC3/IR Observations. *ApJ*, 752:L5, June 2012.

- [17] C. C. Steidel, M. Giavalisco, M. Pettini, M. Dickinson, and K. L. Adelberger. Spectroscopic Confirmation of a Population of Normal Star-forming Galaxies at Redshifts $Z > 3$. *ApJ*, 462:L17, May 1996.
- [18] C. C. Steidel, K. L. Adelberger, A. E. Shapley, M. Pettini, M. Dickinson, and M. Giavalisco. Lyman Break Galaxies at Redshift $z \sim 3$: Survey Description and Full Data Set. *ApJ*, 592:728–754, August 2003.
- [19] E. Vanzella, S. Cristiani, M. Dickinson, M. Giavalisco, H. Kuntschner, J. Haase, M. Nonino, P. Rosati, C. Cesarsky, H. C. Ferguson, R. A. E. Fosbury, A. Grazian, L. A. Moustakas, A. Rettura, P. Popesso, A. Renzini, D. Stern, and GOODS Team. The great observatories origins deep survey. VLT/FORS2 spectroscopy in the GOODS-South field: Part III. *A&A*, 478:83–92, January 2008.
- [20] D. P. Stark, R. S. Ellis, K. Chiu, M. Ouchi, and A. Bunker. Keck spectroscopy of faint $3 < z < 7$ Lyman break galaxies - I. New constraints on cosmic reionization from the luminosity and redshift-dependent fraction of Lyman α emission. *MNRAS*, 408:1628–1648, November 2010.
- [21] P. A. Oesch, P. G. van Dokkum, G. D. Illingworth, R. J. Bouwens, I. Momcheva, B. Holden, G. W. Roberts-Borsani, R. Smit, M. Franx, I. Labbe, V. Gonzalez, and D. Magee. A Spectroscopic Redshift Measurement for a Luminous Lyman Break Galaxy at $z = 7.730$ Using Keck/MOSFIRE. *ApJ*, 804:L30, May 2015.
- [22] R. F. J. van der Burg, H. Hildebrandt, and T. Erben. The UV galaxy luminosity function at $z = 3$ –5 from the CFHT Legacy Survey Deep fields. *A&A*, 523:A74, November 2010.
- [23] S. V. W. Beckwith, M. Stiavelli, A. M. Koekemoer, J. A. R. Caldwell, H. C. Ferguson, R. Hook, R. A. Lucas, L. E. Bergeron, M. Corbin, S. Joge, N. Panagia, M. Robberto, P. Royle, R. S. Somerville, and M. Sosey. The Hubble Ultra Deep Field. *AJ*, 132:1729–1755, November 2006.
- [24] R. J. Bouwens, G. D. Illingworth, P. A. Oesch, I. Labbé, M. Trenti, P. van Dokkum, M. Franx, M. Stiavelli, C. M. Carollo, D. Magee, and V. Gonzalez. Ultraviolet Luminosity Functions from 132 $z \sim 7$ and $z \sim 8$ Lyman-break Galaxies in the Ultra-deep HUDF09 and Wide-area Early Release Science WFC3/IR Observations. *ApJ*, 737:90, August 2011.
- [25] R. S. Ellis, R. J. McLure, J. S. Dunlop, B. E. Robertson, Y. Ono, M. A. Schenker, A. Koekemoer, R. A. A. Bowler, M. Ouchi, A. B. Rogers, E. Curtis-Lake, E. Schneider, S. Charlot, D. P. Stark, S. R. Furlanetto, and M. Cirasuolo. The Abundance of Star-forming Galaxies in the Redshift Range 8.5–12: New Results from the 2012 Hubble Ultra Deep Field Campaign. *ApJ*, 763:L7, January 2013.
- [26] R. J. Bouwens, G. D. Illingworth, M. Franx, and H. Ford. UV Luminosity Functions at $z \sim 4, 5$, and 6 from the Hubble Ultra Deep Field and Other Deep Hubble Space Telescope ACS Fields: Evolution and Star Formation History. *ApJ*, 670:928–958, December 2007.
- [27] M. A. Schenker, B. E. Robertson, R. S. Ellis, Y. Ono, R. J. McLure, J. S. Dunlop, A. Koekemoer, R. A. A. Bowler, M. Ouchi, E. Curtis-Lake, A. B.

- Rogers, E. Schneider, S. Charlot, D. P. Stark, S. R. Furlanetto, and M. Cirasuolo. The UV Luminosity Function of Star-forming Galaxies via Dropout Selection at Redshifts $z \sim 7$ and 8 from the 2012 Ultra Deep Field Campaign. *ApJ*, 768:196, May 2013.
- [28] R. J. McLure, J. S. Dunlop, R. A. A. Bowler, E. Curtis-Lake, M. Schenker, R. S. Ellis, B. E. Robertson, A. M. Koekemoer, A. B. Rogers, Y. Ono, M. Ouchi, S. Charlot, V. Wild, D. P. Stark, S. R. Furlanetto, M. Cirasuolo, and T. A. Targett. A new multifield determination of the galaxy luminosity function at $z = 7-9$ incorporating the 2012 Hubble Ultra-Deep Field imaging. *MNRAS*, 432:2696–2716, July 2013.
- [29] M. Giavalisco, H. C. Ferguson, A. M. Koekemoer, M. Dickinson, D. M. Alexander, F. E. Bauer, J. Bergeron, C. Biagetti, W. N. Brandt, S. Casertano, C. Cesarsky, E. Chatzichristou, C. Conselice, S. Cristiani, L. Da Costa, T. Dahlen, D. de Mello, P. Eisenhardt, T. Erben, S. M. Fall, C. Fassnacht, R. Fosbury, A. Fruchter, J. P. Gardner, N. Grogin, R. N. Hook, A. E. Hornschemeier, R. Idzi, S. Jogee, C. Kretchmer, V. Laidler, K. S. Lee, M. Livio, R. Lucas, P. Madau, B. Mobasher, L. A. Moustakas, M. Nonino, P. Padovani, C. Papovich, Y. Park, S. Ravindranath, A. Renzini, M. Richardson, A. Riess, P. Rosati, M. Schirmer, E. Schreier, R. S. Somerville, H. Spinrad, D. Stern, M. Stiavelli, L. Strolger, C. M. Urry, B. Vandame, R. Williams, and C. Wolf. The Great Observatories Origins Deep Survey: Initial Results from Optical and Near-Infrared Imaging. *ApJ*, 600:L93–L98, January 2004.
- [30] N. A. Grogin, D. D. Kocevski, S. M. Faber, H. C. Ferguson, A. M. Koekemoer, A. G. Riess, V. Acquaviva, D. M. Alexander, O. Almaini, M. L. N. Ashby, M. Barden, E. F. Bell, F. Bournaud, T. M. Brown, K. I. Caputi, S. Casertano, P. Cassata, M. Castellano, P. Challis, R.-R. Chary, E. Cheung, M. Cirasuolo, C. J. Conselice, A. Roshan Cooray, D. J. Croton, E. Daddi, T. Dahlen, R. Davé, D. F. de Mello, A. Dekel, M. Dickinson, T. Dolch, J. L. Donley, J. S. Dunlop, A. A. Dutton, D. Elbaz, G. G. Fazio, A. V. Filippenko, S. L. Finkelstein, A. Fontana, J. P. Gardner, P. M. Garnavich, E. Gawiser, M. Giavalisco, A. Grazian, Y. Guo, N. P. Hathi, B. Häussler, P. F. Hopkins, J.-S. Huang, K.-H. Huang, S. W. Jha, J. S. Kartaltepe, R. P. Kirshner, D. C. Koo, K. Lai, K.-S. Lee, W. Li, J. M. Lotz, R. A. Lucas, P. Madau, P. J. McCarthy, E. J. McGrath, D. H. McIntosh, R. J. McLure, B. Mobasher, L. A. Moustakas, M. Mozena, K. Nandra, J. A. Newman, S.-M. Niemi, K. G. Noeske, C. J. Papovich, L. Pentericci, A. Pope, J. R. Primack, A. Rajan, S. Ravindranath, N. A. Reddy, A. Renzini, H.-W. Rix, A. R. Robaina, S. A. Rodney, D. J. Rosario, P. Rosati, S. Salimbeni, C. Scarlata, B. Siana, L. Simard, J. Smidt, R. S. Somerville, H. Spinrad, A. N. Straughn, L.-G. Strolger, O. Telford, H. I. Teplitz, J. R. Trump, A. van der Wel, C. Villforth, R. H. Wechsler, B. J. Weiner, T. Wiklind, V. Wild, G. Wilson, S. Wuyts, H.-J. Yan, and M. S. Yun. CANDELS: The Cosmic Assembly Near-infrared Deep Extragalactic Legacy Survey. *ApJS*, 197:35, December 2011.
- [31] A. M. Koekemoer, S. M. Faber, H. C. Ferguson, N. A. Grogin, D. D. Kocevski, D. C. Koo, K. Lai, J. M. Lotz, R. A. Lucas, E. J. McGrath, S. Ogaz,

- A. Rajan, A. G. Riess, S. A. Rodney, L. Strolger, S. Casertano, M. Castellano, T. Dahlen, M. Dickinson, T. Dolch, A. Fontana, M. Giavalisco, A. Grazian, Y. Guo, N. P. Hathi, K.-H. Huang, A. van der Wel, H.-J. Yan, V. Acquaviva, D. M. Alexander, O. Almaini, M. L. N. Ashby, M. Barden, E. F. Bell, F. Bournaud, T. M. Brown, K. I. Caputi, P. Cassata, P. J. Challis, R.-R. Chary, E. Cheung, M. Cirasuolo, C. J. Conselice, A. Roshan Cooray, D. J. Croton, E. Daddi, R. Davé, D. F. de Mello, L. de Ravel, A. Dekel, J. L. Donley, J. S. Dunlop, A. A. Dutton, D. Elbaz, G. G. Fazio, A. V. Filippenko, S. L. Finkelstein, C. Frazer, J. P. Gardner, P. M. Garnavich, E. Gawiser, R. Gruetzbauch, W. G. Hartley, B. Häussler, J. Herrington, P. F. Hopkins, J.-S. Huang, S. W. Jha, A. Johnson, J. S. Kartaltepe, A. A. Khostovan, R. P. Kirshner, C. Lani, K.-S. Lee, W. Li, P. Madau, P. J. McCarthy, D. H. McIntosh, R. J. McLure, C. McPartland, B. Mobasher, H. Moreira, A. Mortlock, L. A. Moustakas, M. Mozena, K. Nandra, J. A. Newman, J. L. Nielsen, S. Niemi, K. G. Noeske, C. J. Papovich, L. Pentericci, A. Pope, J. R. Primack, S. Ravindranath, N. A. Reddy, A. Renzini, H.-W. Rix, A. R. Robaina, D. J. Rosario, P. Rosati, S. Salimbeni, C. Scarlata, B. Siana, L. Simard, J. Smidt, D. Snyder, R. S. Somerville, H. Spinrad, A. N. Straughn, O. Telford, H. I. Teplitz, J. R. Trump, C. Vargas, C. Villforth, C. R. Wagner, P. Wandro, R. H. Wechsler, B. J. Weiner, T. Wiklind, V. Wild, G. Wilson, S. Wuyts, and M. S. Yun. CANDELS: The Cosmic Assembly Near-infrared Deep Extragalactic Legacy Survey – The Hubble Space Telescope Observations, Imaging Data Products, and Mosaics. *ApJS*, 197:36, December 2011.
- [32] H. J. McCracken, B. Milvang-Jensen, J. Dunlop, M. Franx, J. P. U. Fynbo, O. Le Fèvre, J. Holt, K. I. Caputi, Y. Goranova, F. Buitrago, J. P. Emerson, W. Freudling, P. Hudelot, C. López-Sanjuan, F. Magnard, Y. Mellier, P. Møller, K. K. Nilsson, W. Sutherland, L. Tasca, and J. Zabl. UltraVISTA: a new ultra-deep near-infrared survey in COSMOS. *A&A*, 544:A156, August 2012.
- [33] C. J. Willott, R. J. McLure, P. Hibon, R. Bielby, H. J. McCracken, J.-P. Kneib, O. Ilbert, D. G. Bonfield, V. A. Bruce, and M. J. Jarvis. An Exponential Decline at the Bright End of the $z = 6$ Galaxy Luminosity Function. *AJ*, 145:4, January 2013.
- [34] S. L. Finkelstein, R. E. Ryan, Jr., C. Papovich, M. Dickinson, M. Song, R. Somerville, H. C. Ferguson, B. Salmon, M. Giavalisco, A. M. Koekemoer, M. L. N. Ashby, P. Behroozi, M. Castellano, J. S. Dunlop, S. M. Faber, G. G. Fazio, A. Fontana, N. A. Grogan, N. Hathi, J. Jaacks, D. D. Kocevski, R. Livermore, R. J. McLure, E. Merlin, B. Mobasher, J. A. Newman, M. Rafelski, V. Tilvi, and S. P. Willner. The Evolution of the Galaxy Rest-Frame Ultraviolet Luminosity Function Over the First Two Billion Years. *ArXiv e-prints*, October 2014.
- [35] R. A. A. Bowler, J. S. Dunlop, R. J. McLure, A. B. Rogers, H. J. McCracken, B. Milvang-Jensen, H. Furusawa, J. P. U. Fynbo, Y. Taniguchi, J. Afonso, M. N. Bremer, and O. Le Fèvre. The bright end of the galaxy luminosity function at $z \sim 7$: before the onset of mass quenching? *MNRAS*, 440:2810–

- 2842, May 2014.
- [36] R. A. A. Bowler, J. S. Dunlop, R. J. McLure, H. J. McCracken, H. Furusawa, Y. Taniguchi, J. P. U. Fynbo, B. Milvang-Jensen, and O. Le Fevre. The galaxy luminosity function at $z \sim 6$ and evidence for rapid evolution in the bright end from $z \sim 7$ to 5. *ArXiv e-prints*, November 2014.
 - [37] R. J. Bouwens, G. D. Illingworth, M. Franx, and H. Ford. $z \sim 7$ -10 Galaxies in the HUDF and GOODS Fields: UV Luminosity Functions. *ApJ*, 686:230–250, October 2008.
 - [38] N. A. Reddy and C. C. Steidel. A Steep Faint-End Slope of the UV Luminosity Function at $z \sim 2$ -3: Implications for the Global Stellar Mass Density and Star Formation in Low-Mass Halos. *ApJ*, 692:778–803, February 2009.
 - [39] C. C. Steidel, K. L. Adelberger, M. Giavalisco, M. Dickinson, and M. Pettini. Lyman-Break Galaxies at $z \geq 4$ and the Evolution of the Ultraviolet Luminosity Density at High Redshift. *ApJ*, 519:1–17, July 1999.
 - [40] S. Arnouts, D. Schiminovich, O. Ilbert, L. Tresse, B. Milliard, M. Treyer, S. Bardelli, T. Budavari, T. K. Wyder, E. Zucca, O. Le Fèvre, D. C. Martin, G. Vettolani, C. Adami, M. Arnaboldi, T. Barlow, L. Bianchi, M. Bolzonella, D. Bottini, Y.-I. Byun, A. Cappi, S. Charlot, T. Contini, J. Donas, K. Forster, S. Foucaud, P. Franzetti, P. G. Friedman, B. Garilli, I. Gavignaud, L. Guzzo, T. M. Heckman, C. Hoopes, A. Iovino, P. Jelinsky, V. Le Brun, Y.-W. Lee, D. Maccagni, B. F. Madore, R. Malina, B. Marano, C. Marinoni, H. J. McCracken, A. Mazure, B. Meneux, R. Merighi, P. Morrissey, S. Neff, S. Paltani, R. Pellò, J. P. Picat, A. Pollo, L. Pozzetti, M. Radovich, R. M. Rich, R. Scaramella, M. Scodeggio, M. Seibert, O. Siegmund, T. Small, A. S. Szalay, B. Welsh, C. K. Xu, G. Zamorani, and A. Zanichelli. The GALEX VIMOS-VLT Deep Survey Measurement of the Evolution of the 1500 Å Luminosity Function. *ApJ*, 619:L43–L46, January 2005.
 - [41] P. A. Oesch, R. J. Bouwens, C. M. Carollo, G. D. Illingworth, D. Magee, M. Trenti, M. Stiavelli, M. Franx, I. Labbé, and P. G. van Dokkum. The Evolution of the Ultraviolet Luminosity Function from $z \sim 0.75$ to $z \sim 2.5$ Using HST ERS WFC3/UVIS Observations. *ApJ*, 725:L150–L155, December 2010.
 - [42] H. Yan and R. A. Windhorst. Candidates of $z \sim 5.5$ -7 Galaxies in the Hubble Space Telescope Ultra Deep Field. *ApJ*, 612:L93–L96, September 2004.
 - [43] M. Trenti, L. D. Bradley, M. Stiavelli, P. Oesch, T. Treu, R. J. Bouwens, J. M. Shull, J. W. MacKenty, C. M. Carollo, and G. D. Illingworth. The Brightest of Reionizing Galaxies Survey: Design and Preliminary Results. *ApJ*, 727:L39, February 2011.
 - [44] H. Yan, L. Yan, M. A. Zamojski, R. A. Windhorst, P. J. McCarthy, X. Fan, H. J. A. Röttgering, A. M. Koekemoer, B. E. Robertson, R. Davé, and Z. Cai. Probing Very Bright End of Galaxy Luminosity Function at $z > 7$ Using Hubble Space Telescope Pure Parallel Observations. *ApJ*, 728:L22, February 2011.
 - [45] R. J. Bouwens, G. D. Illingworth, P. A. Oesch, I. Labbé, P. G. van Dokkum, M. Trenti, M. Franx, R. Smit, V. Gonzalez, and D. Magee. UV-continuum

- Slopes of >4000 $z \sim 4$ -8 Galaxies from the HUDF/XDF, HUDF09, ERS, CANDELS-South, and CANDELS-North Fields. *ApJ*, 793:115, October 2014.
- [46] R. J. Bouwens, G. D. Illingworth, P. A. Oesch, M. Franx, I. Labbé, M. Trenti, P. van Dokkum, C. M. Carollo, V. González, R. Smit, and D. Magee. UV-continuum Slopes at $z \sim 4$ -7 from the HUDF09+ERS+CANDELS Observations: Discovery of a Well-defined UV Color-Magnitude Relationship for $z \geq 4$ Star-forming Galaxies. *ApJ*, 754:83, August 2012.
 - [47] A. B. Rogers, R. J. McLure, J. S. Dunlop, R. A. A. Bowler, E. F. Curtis-Lake, P. Dayal, S. M. Faber, H. C. Ferguson, S. L. Finkelstein, N. A. Grogin, N. P. Hathi, D. Kocevski, A. M. Koekemoer, and P. Kurczynski. The colour distribution of galaxies at redshift five. *MNRAS*, 440:3714–3725, June 2014.
 - [48] G. R. Meurer, T. M. Heckman, and D. Calzetti. Dust Absorption and the Ultraviolet Luminosity Density at $z \sim 3$ as Calibrated by Local Starburst Galaxies. *ApJ*, 521:64–80, August 1999.
 - [49] K. L. Adelberger and C. C. Steidel. Multiwavelength Observations of Dusty Star Formation at Low and High Redshift. *ApJ*, 544:218–241, November 2000.
 - [50] E. R. Stanway, R. G. McMahon, and A. J. Bunker. Near-infrared properties of i-drop galaxies in the Hubble Ultra Deep Field. *MNRAS*, 359:1184–1192, May 2005.
 - [51] R. J. Bouwens, G. D. Illingworth, M. Franx, R.-R. Chary, G. R. Meurer, C. J. Conselice, H. Ford, M. Giavalisco, and P. van Dokkum. UV Continuum Slope and Dust Obscuration from $z \sim 6$ to $z \sim 2$: The Star Formation Rate Density at High Redshift. *ApJ*, 705:936–961, November 2009.
 - [52] S. M. Wilkins, A. J. Bunker, E. Stanway, S. Lorenzoni, and J. Caruana. The ultraviolet properties of star-forming galaxies - I. HST WFC3 observations of very high redshift galaxies. *MNRAS*, 417:717–729, October 2011.
 - [53] M. Castellano, A. Fontana, A. Grazian, L. Pentericci, P. Santini, A. Koekemoer, S. Cristiani, A. Galametz, S. Gallerani, E. Vanzella, K. Boutsia, S. Gallozzi, E. Giallongo, R. Maiolino, N. Menci, and D. Paris. The blue UV slopes of $z \sim 4$ Lyman break galaxies: implications for the corrected star formation rate density. *A&A*, 540:A39, April 2012.
 - [54] J. S. Dunlop, R. J. McLure, B. E. Robertson, R. S. Ellis, D. P. Stark, M. Cirasuolo, and L. de Ravel. A critical analysis of the ultraviolet continuum slopes (β) of high-redshift galaxies: no evidence (yet) for extreme stellar populations at $z > 6$. *MNRAS*, 420:901–912, February 2012.
 - [55] S. L. Finkelstein, C. Papovich, B. Salmon, K. Finlator, M. Dickinson, H. C. Ferguson, M. Giavalisco, A. M. Koekemoer, N. A. Reddy, R. Bassett, C. J. Conselice, J. S. Dunlop, S. M. Faber, N. A. Grogin, N. P. Hathi, D. D. Kocevski, K. Lai, K.-S. Lee, R. J. McLure, B. Mobasher, and J. A. Newman. Candels: The Evolution of Galaxy Rest-frame Ultraviolet Colors from $z = 8$ to 4. *ApJ*, 756:164, September 2012.
 - [56] N. P. Hathi, S. H. Cohen, R. E. Ryan, Jr., S. L. Finkelstein, P. J. McCarthy, R. A. Windhorst, H. Yan, A. M. Koekemoer, M. J. Rutkowski, R. W.

- O’Connell, A. N. Straughn, B. Balick, H. E. Bond, D. Calzetti, M. J. Disney, M. A. Dopita, J. A. Frogel, D. N. B. Hall, J. A. Holtzman, R. A. Kimble, F. Paresce, A. Saha, J. I. Silk, J. T. Trauger, A. R. Walker, B. C. Whitmore, and E. T. Young. Stellar Populations of Lyman Break Galaxies at $z \sim 1-3$ in the HST/WFC3 Early Release Science Observations. *ApJ*, 765:88, March 2013.
- [57] P. Kurczynski, E. Gawiser, M. Rafelski, H. I. Teplitz, V. Acquaviva, T. M. Brown, D. Coe, D. F. de Mello, S. L. Finkelstein, N. A. Gugin, A. M. Koekemoer, K.-S. Lee, C. Scarlata, and B. D. Siana. The UV Continuum of $z > 1$ Star-forming Galaxies in the Hubble Ultraviolet UltraDeep Field. *ApJ*, 793:L5, September 2014.
- [58] S. M. Wilkins, A. Bunker, W. Coulton, R. Croft, T. D. Matteo, N. Khandai, and Y. Feng. Interpreting the observed UV continuum slopes of high-redshift galaxies. *MNRAS*, 430:2885–2890, April 2013.
- [59] K. Finlator, B. D. Oppenheimer, and R. Davé. Smoothly rising star formation histories during the reionization epoch. *MNRAS*, 410:1703–1724, January 2011.
- [60] G. Bruzual and S. Charlot. Stellar population synthesis at the resolution of 2003. *MNRAS*, 344:1000–1028, October 2003.
- [61] S. Charlot and S. M. Fall. A Simple Model for the Absorption of Starlight by Dust in Galaxies. *ApJ*, 539:718–731, August 2000.
- [62] B. E. Robertson, S. R. Furlanetto, E. Schneider, S. Charlot, R. S. Ellis, D. P. Stark, R. J. McLure, J. S. Dunlop, A. Koekemoer, M. A. Schenker, M. Ouchi, Y. Ono, E. Curtis-Lake, A. B. Rogers, R. A. A. Bowler, and M. Cirasuolo. New Constraints on Cosmic Reionization from the 2012 Hubble Ultra Deep Field Campaign. *ApJ*, 768:71, May 2013.
- [63] J. S. Dunlop, A. B. Rogers, R. J. McLure, R. S. Ellis, B. E. Robertson, A. Koekemoer, P. Dayal, E. Curtis-Lake, V. Wild, S. Charlot, R. A. A. Bowler, M. A. Schenker, M. Ouchi, Y. Ono, M. Cirasuolo, S. R. Furlanetto, D. P. Stark, T. A. Targett, and E. Schneider. The UV continua and inferred stellar populations of galaxies at $z \sim 7-9$ revealed by the Hubble Ultra-Deep Field 2012 campaign. *MNRAS*, 432:3520–3533, July 2013.
- [64] M. Kuhlen and C.-A. Faucher-Giguère. Concordance models of reionization: implications for faint galaxies and escape fraction evolution. *MNRAS*, 423:862–876, June 2012.
- [65] P. Madau, F. Haardt, and M. J. Rees. Radiative Transfer in a Clumpy Universe. III. The Nature of Cosmological Ionizing Sources. *ApJ*, 514:648–659, April 1999.
- [66] C. Leitherer, H. C. Ferguson, T. M. Heckman, and J. D. Lowenthal. The Lyman Continuum in Starburst Galaxies Observed with the Hopkins Ultraviolet Telescope. *ApJ*, 454:L19, November 1995.
- [67] J.-M. Deharveng, V. Buat, V. Le Brun, B. Milliard, D. Kunth, J. M. Shull, and C. Gry. Constraints on the Lyman continuum radiation from galaxies: First results with FUSE on Mrk 54. *A&A*, 375:805–813, September 2001.

- [68] E. Giallongo, S. Cristiani, S. D’Odorico, and A. Fontana. A Low Upper Limit to the Lyman Continuum Emission of Two Galaxies at $z \sim 3$. *ApJ*, 568:L9–L12, March 2002.
- [69] M. Malkan, W. Webb, and Q. Konopacky. A Hubble Space Telescope Search for Lyman Continuum Emission from Galaxies at $1.1 < z < 1.4$. *ApJ*, 598:878–885, December 2003.
- [70] B. Siana, H. I. Teplitz, J. Colbert, H. C. Ferguson, M. Dickinson, T. M. Brown, C. J. Conselice, D. F. de Mello, J. P. Gardner, M. Giavalisco, and F. Menanteau. New Constraints on the Lyman Continuum Escape Fraction at $z \sim 1.3$. *ApJ*, 668:62–73, October 2007.
- [71] J. P. Grimes, T. Heckman, D. Strickland, W. V. Dixon, K. Sembach, R. Overzier, C. Hoopes, A. Aloisi, and A. Ptak. Feedback in the Local Lyman-break Galaxy Analog Haro 11 as Probed by Far-Ultraviolet and X-Ray Observations. *ApJ*, 668:891–905, October 2007.
- [72] L. L. Cowie, A. J. Barger, and L. Trouille. Measuring the Sources of the Intergalactic Ionizing Flux. *ApJ*, 692:1476–1488, February 2009.
- [73] B. Siana, H. I. Teplitz, H. C. Ferguson, T. M. Brown, M. Giavalisco, M. Dickinson, R.-R. Chary, D. F. de Mello, C. J. Conselice, C. R. Bridge, J. P. Gardner, J. W. Colbert, and C. Scarlata. A Deep Hubble Space Telescope Search for Escaping Lyman Continuum Flux at $z \sim 1.3$: Evidence for an Evolving Ionizing Emissivity. *ApJ*, 723:241–250, November 2010.
- [74] T. M. Heckman, S. Borthakur, R. Overzier, G. Kauffmann, A. Basu-Zych, C. Leitherer, K. Sembach, D. C. Martin, R. M. Rich, D. Schiminovich, and M. Seibert. Extreme Feedback and the Epoch of Reionization: Clues in the Local Universe. *ApJ*, 730:5, March 2011.
- [75] E. Vanzella, Y. Guo, M. Giavalisco, A. Grazian, M. Castellano, S. Cristiani, M. Dickinson, A. Fontana, M. Nonino, E. Giallongo, L. Pentericci, A. Galametz, S. M. Faber, H. C. Ferguson, N. A. Grogin, A. M. Koekemoer, J. Newman, and B. D. Siana. On the Detection of Ionizing Radiation Arising from Star-forming Galaxies at Redshift $z \sim 3-4$: Looking for Analogs of “Stellar Re-ionizers”. *ApJ*, 751:70, May 2012.
- [76] D. B. Nestor, A. E. Shapley, K. A. Kornei, C. C. Steidel, and B. Siana. A Refined Estimate of the Ionizing Emissivity from Galaxies at $z \sim 3$: Spectroscopic Follow-up in the SSA22a Field. *ApJ*, 765:47, March 2013.
- [77] J. Cooke, E. V. Ryan-Weber, T. Garel, and C. G. Díaz. Lyman-continuum galaxies and the escape fraction of Lyman-break galaxies. *MNRAS*, 441:837–851, June 2014.
- [78] B. Siana, A. E. Shapley, K. R. Kulas, D. B. Nestor, C. C. Steidel, H. I. Teplitz, A. Alavi, T. M. Brown, C. J. Conselice, H. C. Ferguson, M. Dickinson, M. Giavalisco, J. W. Colbert, C. R. Bridge, J. P. Gardner (GSFC), and D. F. de Mello (Catholic University). A Deep Hubble Space Telescope and Keck Search for Definitive Identification of Lyman Continuum Emitters at $z \sim 3.1$. *ApJ*, 804:17, May 2015.

- [79] D. B. Nestor, A. E. Shapley, C. C. Steidel, and B. Siana. Narrowband Imaging of Escaping Lyman-continuum Emission in the SSA22 Field. *ApJ*, 736:18, July 2011.
- [80] C. C. Steidel, M. Pettini, and K. L. Adelberger. Lyman-Continuum Emission from Galaxies at $Z \sim 3.4$. *ApJ*, 546:665–671, January 2001.
- [81] M. Hayes, D. Schaerer, G. Östlin, J. M. Mas-Hesse, H. Atek, and D. Kunth. On the Redshift Evolution of the $\text{Ly}\alpha$ Escape Fraction and the Dust Content of Galaxies. *ApJ*, 730:8, March 2011.
- [82] T. A. Jones, R. S. Ellis, M. A. Schenker, and D. P. Stark. Keck Spectroscopy of Gravitationally Lensed $z \sim 4$ Galaxies: Improved Constraints on the Escape Fraction of Ionizing Photons. *ApJ*, 779:52, December 2013.
- [83] F. Haardt and P. Madau. Radiative Transfer in a Clumpy Universe. IV. New Synthesis Models of the Cosmic UV/X-Ray Background. *ApJ*, 746:125, February 2012.
- [84] C.-A. Faucher-Giguère, A. Lidz, L. Hernquist, and M. Zaldarriaga. Evolution of the Intergalactic Opacity: Implications for the Ionizing Background, Cosmic Star Formation, and Quasar Activity. *ApJ*, 688:85–107, November 2008.
- [85] A. Songaila and L. L. Cowie. The Evolution of Lyman Limit Absorption Systems to Redshift Six. *ApJ*, 721:1448–1466, October 2010.
- [86] H.-W. Chen, J. X. Prochaska, and N. Y. Gnedin. A New Constraint on the Escape Fraction in Distant Galaxies Using γ -Ray Burst Afterglow Spectroscopy. *ApJ*, 667:L125–L128, October 2007.
- [87] D. Calzetti, L. Armus, R. C. Bohlin, A. L. Kinney, J. Koornneef, and T. Storchi-Bergmann. The Dust Content and Opacity of Actively Star-forming Galaxies. *ApJ*, 533:682–695, April 2000.
- [88] J. A. Muñoz and A. Loeb. Constraining the Minimum Mass of High-redshift Galaxies and their Contribution to the Ionization State of the Intergalactic Medium. *ApJ*, 729:99, March 2011.
- [89] A. Alavi, B. Siana, J. Richard, D. P. Stark, C. Scarlata, H. I. Teplitz, W. R. Freeman, A. Dominguez, M. Rafelski, B. Robertson, and L. Kewley. Ultra-faint Ultraviolet Galaxies at $z \sim 2$ behind the Lensing Cluster A1689: The Luminosity Function, Dust Extinction, and Star Formation Rate Density. *ApJ*, 780:143, January 2014.
- [90] M. Sawicki and D. Thompson. Keck Deep Fields. II. The Ultraviolet Galaxy Luminosity Function at $z \sim 4, 3$, and 2. *ApJ*, 642:653–672, May 2006.
- [91] N. P. Hathi, R. E. Ryan, Jr., S. H. Cohen, H. Yan, R. A. Windhorst, P. J. McCarthy, R. W. O’Connell, A. M. Koekemoer, M. J. Rutkowski, B. Balick, H. E. Bond, D. Calzetti, M. J. Disney, M. A. Dopita, J. A. Frogel, D. N. B. Hall, J. A. Holtzman, R. A. Kimble, F. Paresce, A. Saha, J. I. Silk, J. T. Trauger, A. R. Walker, B. C. Whitmore, and E. T. Young. UV-dropout Galaxies in the GOODS-South Field from WFC3 Early Release Science Observations. *ApJ*, 720:1708–1716, September 2010.
- [92] J. I. Read, A. P. Pontzen, and M. Viel. On the formation of dwarf galaxies and stellar haloes. *MNRAS*, 371:885–897, September 2006.

- [93] M. J. Rees and J. P. Ostriker. Cooling, dynamics and fragmentation of massive gas clouds - Clues to the masses and radii of galaxies and clusters. *MNRAS*, 179:541–559, June 1977.
- [94] M.-M. Mac Low and A. Ferrara. Starburst-driven Mass Loss from Dwarf Galaxies: Efficiency and Metal Ejection. *ApJ*, 513:142–155, March 1999.
- [95] M. Dijkstra, Z. Haiman, M. J. Rees, and D. H. Weinberg. Photoionization Feedback in Low-Mass Galaxies at High Redshift. *ApJ*, 601:666–675, February 2004.
- [96] D. R. Weisz, B. D. Johnson, and C. Conroy. The Very Faint End of the UV Luminosity Function over Cosmic Time: Constraints from the Local Group Fossil Record. *ApJ*, 794:L3, October 2014.
- [97] B. W. O’Shea, J. H. Wise, H. Xu, and M. L. Norman. The Ultraviolet Luminosity Function of the Earliest Galaxies. *ArXiv e-prints*, March 2015.
- [98] R. J. Bouwens, G. D. Illingworth, I. Labbe, P. A. Oesch, M. Trenti, C. M. Carollo, P. G. van Dokkum, M. Franx, M. Stiavelli, V. González, D. Magee, and L. Bradley. A candidate redshift $z \sim 10$ galaxy and rapid changes in that population at an age of 500 Myr. *Nature*, 469:504–507, January 2011.
- [99] P. A. Oesch, R. J. Bouwens, G. D. Illingworth, I. Labbé, M. Trenti, V. Gonzalez, C. M. Carollo, M. Franx, P. G. van Dokkum, and D. Magee. Expanded Search for $z \sim 10$ Galaxies from HUDF09, ERS, and CANDELS Data: Evidence for Accelerated Evolution at $z > 8$? *ApJ*, 745:110, February 2012.
- [100] P. A. Oesch, R. J. Bouwens, G. D. Illingworth, I. Labbé, M. Franx, P. G. van Dokkum, M. Trenti, M. Stiavelli, V. Gonzalez, and D. Magee. Probing the Dawn of Galaxies at $z \sim 9$ –12: New Constraints from HUDF12/XDF and CANDELS data. *ApJ*, 773:75, August 2013.
- [101] M. Trenti, M. Stiavelli, R. J. Bouwens, P. Oesch, J. M. Shull, G. D. Illingworth, L. D. Bradley, and C. M. Carollo. The Galaxy Luminosity Function During the Reionization Epoch. *ApJ*, 714:L202–L207, May 2010.
- [102] C. G. Lacey, C. M. Baugh, C. S. Frenk, and A. J. Benson. The evolution of Lyman-break galaxies in the cold dark matter model. *MNRAS*, 412:1828–1852, April 2011.
- [103] S. Tacchella, M. Trenti, and C. M. Carollo. A Physical Model for the $0 < z < 8$ Redshift Evolution of the Galaxy Ultraviolet Luminosity and Stellar Mass Functions. *ApJ*, 768:L37, May 2013.
- [104] S. Genel, M. Vogelsberger, V. Springel, D. Sijacki, D. Nelson, G. Snyder, V. Rodriguez-Gomez, P. Torrey, and L. Hernquist. Introducing the Illustris project: the evolution of galaxy populations across cosmic time. *MNRAS*, 445:175–200, November 2014.
- [105] P. S. Behroozi and J. Silk. A Simple Technique for Predicting High-redshift Galaxy Evolution. *ApJ*, 799:32, January 2015.
- [106] R. Smit, R. J. Bouwens, M. Franx, G. D. Illingworth, I. Labbé, P. A. Oesch, and P. G. van Dokkum. The Star Formation Rate Function for Redshift $z \sim 4$ –7 Galaxies: Evidence for a Uniform Buildup of Star-forming Galaxies during the First 3 Gyr of Cosmic Time. *ApJ*, 756:14, September 2012.

- [107] R. J. Bouwens, L. Bradley, A. Zitrin, D. Coe, M. Franx, W. Zheng, R. Smit, O. Host, M. Postman, L. Moustakas, I. Labbé, M. Carrasco, A. Molino, M. Donahue, D. D. Kelson, M. Meneghetti, N. Benítez, D. Lemze, K. Umetsu, T. Broadhurst, J. Moustakas, P. Rosati, S. Jouvel, M. Bartelmann, H. Ford, G. Graves, C. Grillo, L. Infante, Y. Jimenez-Teja, O. Lahav, D. Maoz, E. Medezinski, P. Melchior, J. Merten, M. Nonino, S. Ogaz, and S. Seitz. A Census of Star-forming Galaxies in the $Z \sim 9$ -10 Universe based on HST+Spitzer Observations over 19 Clash Clusters: Three Candidate $Z \sim 9$ -10 Galaxies and Improved Constraints on the Star Formation Rate Density at $Z \sim 9.2$. *ApJ*, 795:126, November 2014.
- [108] W. Zheng, M. Postman, A. Zitrin, J. Moustakas, X. Shu, S. Jouvel, O. Høst, A. Molino, L. Bradley, D. Coe, L. A. Moustakas, M. Carrasco, H. Ford, N. Benítez, T. R. Lauer, S. Seitz, R. Bouwens, A. Koekemoer, E. Medezinski, M. Bartelmann, T. Broadhurst, M. Donahue, C. Grillo, L. Infante, S. W. Jha, D. D. Kelson, O. Lahav, D. Lemze, P. Melchior, M. Meneghetti, J. Merten, M. Nonino, S. Ogaz, P. Rosati, K. Umetsu, and A. van der Wel. A magnified young galaxy from about 500 million years after the Big Bang. *Nature*, 489:406–408, September 2012.
- [109] D. Coe, A. Zitrin, M. Carrasco, X. Shu, W. Zheng, M. Postman, L. Bradley, A. Koekemoer, R. Bouwens, T. Broadhurst, A. Monna, O. Host, L. A. Moustakas, H. Ford, J. Moustakas, A. van der Wel, M. Donahue, S. A. Rodney, N. Benítez, S. Jouvel, S. Seitz, D. D. Kelson, and P. Rosati. CLASH: Three Strongly Lensed Images of a Candidate $z \approx 11$ Galaxy. *ApJ*, 762:32, January 2013.
- [110] A. Zitrin, W. Zheng, T. Broadhurst, J. Moustakas, D. Lam, X. Shu, X. Huang, J. M. Diego, H. Ford, J. Lim, F. E. Bauer, L. Infante, D. D. Kelson, and A. Molino. A Geometrically Supported $z \sim 10$ Candidate Multiply Imaged by the Hubble Frontier Fields Cluster A2744. *ApJ*, 793:L12, September 2014.
- [111] P. A. Oesch, R. J. Bouwens, G. D. Illingworth, M. Franx, S. M. Ammons, P. G. van Dokkum, M. Trenti, and I. Labbe. First Frontier Field Constraints on the Cosmic Star-Formation Rate Density at $z \sim 10$ - The Impact of Lensing Shear on Completeness of High-Redshift Galaxy Samples. *ArXiv e-prints*, September 2014.
- [112] D. J. McLeod, R. J. McLure, J. S. Dunlop, B. E. Robertson, R. S. Ellis, and T. T. Targett. New redshift $z > \sim 9$ galaxies in the Hubble Frontier Fields: implications for early evolution of the UV luminosity density. *MNRAS*, 450:3032–3044, July 2015.
- [113] D. Coe, L. Bradley, and A. Zitrin. Frontier Fields: High-redshift Predictions and Early Results. *ApJ*, 800:84, February 2015.
- [114] G. D. Becker and J. S. Bolton. New measurements of the ionizing ultraviolet background over $2 < z < 5$ and implications for hydrogen reionization. *MNRAS*, 436:1023–1039, December 2013.
- [115] R. E. Mostardi, A. E. Shapley, D. B. Nestor, C. C. Steidel, N. A. Reddy, and R. F. Trainor. Narrowband Lyman-continuum Imaging of Galaxies at $z \sim 2.85$. *ApJ*, 779:65, December 2013.

- [116] B. E. Robertson, R. S. Ellis, S. R. Furlanetto, and J. S. Dunlop. Cosmic Reionization and Early Star-forming Galaxies: A Joint Analysis of New Constraints from Planck and the Hubble Space Telescope. *ApJ*, 802:L19, April 2015.
- [117] L. Hui and Z. Haiman. The Thermal Memory of Reionization History. *ApJ*, 596:9–18, October 2003.
- [118] T. R. Choudhury and A. Ferrara. Experimental constraints on self-consistent reionization models. *MNRAS*, 361:577–594, August 2005.
- [119] J. S. Bolton and M. G. Haehnelt. The observed ionization rate of the intergalactic medium and the ionizing emissivity at $z \geq 5$: evidence for a photon-starved and extended epoch of reionization. *MNRAS*, 382:325–341, November 2007.
- [120] P. A. Oesch, C. M. Carollo, M. Stiavelli, M. Trenti, L. E. Bergeron, A. M. Koekemoer, R. A. Lucas, C. M. Pavlovsky, S. V. W. Beckwith, T. Dahlen, H. C. Ferguson, J. P. Gardner, S. J. Lilly, B. Mobasher, and N. Panagia. The UDF05 Follow-Up of the Hubble Ultra Deep Field. II. Constraints on Reionization from Z-Dropout Galaxies. *ApJ*, 690:1350–1357, January 2009.
- [121] M. A. Alvarez, K. Finlator, and M. Trenti. Constraints on the Ionizing Efficiency of the First Galaxies. *ApJ*, 759:L38, November 2012.
- [122] Z.-Y. Cai, A. Lapi, A. Bressan, G. De Zotti, M. Negrello, and L. Danese. A Physical Model for the Evolving Ultraviolet Luminosity Function of High Redshift Galaxies and their Contribution to the Cosmic Reionization. *ApJ*, 785:65, April 2014.
- [123] T. R. Choudhury, E. Puchwein, M. G. Haehnelt, and J. S. Bolton. Lyman- α emitters gone missing: evidence for late reionization? *ArXiv e-prints*, December 2014.
- [124] E. Sobacchi and A. Mesinger. Inhomogeneous recombinations during cosmic reionization. *MNRAS*, 440:1662–1673, May 2014.
- [125] R. J. Bouwens, G. D. Illingworth, P. A. Oesch, J. Caruana, B. Holwerda, R. Smit, and S. Wilkins. Cosmic Reionization after Planck: The Derived Growth of the Cosmic Ionizing Emissivity now matches the Growth of the Galaxy UV Luminosity Density. *ArXiv e-prints*, March 2015.
- [126] M. A. Schenker, R. S. Ellis, N. P. Konidaris, and D. P. Stark. Line-emitting Galaxies beyond a Redshift of 7: An Improved Method for Estimating the Evolving Neutrality of the Intergalactic Medium. *ApJ*, 795:20, November 2014.
- [127] S. Mitra, T. R. Choudhury, and A. Ferrara. Cosmic Reionization after Planck. *ArXiv e-prints*, May 2015.
- [128] G. D. Illingworth, D. Magee, P. A. Oesch, R. J. Bouwens, I. Labbé, M. Stiavelli, P. G. van Dokkum, M. Franx, M. Trenti, C. M. Carollo, and V. Gonzalez. The HST eXtreme Deep Field (XDF): Combining All ACS and WFC3/IR Data on the HUDF Region into the Deepest Field Ever. *ApJS*, 209:6, November 2013.